Developing effective subsoil reference model for seismic microzonation studies: Central Italy case studies

Published:
DOI: http://doi.org/10.1007/s11069-021-05188-5

DEVELOPING EFFECTIVE SUBSOIL REFERENCE MODEL FOR SEISMIC MICROZONATION STUDIES: CENTRAL ITALY CASE STUDIES

Pierluigi Pieruccini[1], Enrico Paolucci[2], Pier Lorenzo Fantozzi[2], Duccio Naldini[2], Dario Albarello[2,3]

[1]Dipartimento di Scienze della Terra, Università degli Studi di Torino, Via Valperga Caluso 35, 10125 Turin, Italy
[2]Dipartimento di Scienze Fisiche, della Terra e dell'Ambiente, Università degli Studi di Siena, Via Laterina 8, 53100 Siena, Italy
[3]Istituto di Geologia Ambientale e Geoingegneria (IGAG), Consiglio Nazionale delle Ricerche (CNR), Area della Ricerca di Roma 1, Montelibretti, Italy

Corresponding Author: Dario Albarello
E-mail address: dario.albarello@unisi.it

Keywords: Seismic Microzonation, Engineering-Geological Model, site effects, Amplification Factors

Abstract

A general methodological approach is here discussed to integrate geological and geophysical information in seismic microzonation studies. In particular, the methodology aims at maximizing the exploitation of low-cost data for extensive preliminary assessment of ground motion amplification phenomena induced by the local seismostratigraphical configuration. Three main steps are delineated: a) the combination of geological/geomorphological analyses to develop an Engineering-Geological Model of the study area; b) targeted geophysical prospecting to provide an Engineering-Geological/Geophysical Model; c) evaluating effectiveness of Engineering-Geological/Geophysical Model by estimating expected ground motion amplification phenomena by the use of suitable computational tools. The workflow is illustrated by a case-study based on a set of villages in the Umbro-Marchean Apennine (Central Italy) damaged during the Seismic sequence occurred in Central Italy during 2016-2017.

1. INTRODUCTION

Since the pioneering studies by Baratta (1910) after 1908 Messina Earthquake the significant role of the local geological-geomorphological setting in controlling the distribution of damages induced by the seismic ground motion became an important issue later formalized by Medvedev (1965) for seismic hazard assessment at local scale (Faccioli, 1986). More recently, theoretical modeling and experimental data put in evidence that the relationships between ground shaking and geological-geomorphological settings relies on the presence and geometry of sharp variations in the elastic properties of rocks (seismic impedance contrasts) and associated shear waves velocity (Vs) variations are responsible for seismic energy trapping and resonance phenomena in the shallowest part of the subsurface and relative interference phenomena of engineering interest (e.g., Kramer, 1996).
The most recent seismic codes (e.g., BSSC NHERP, 2000; EN 1998-1, 2004) implement this view to account for possible ground motion amplification phenomena in the anti-seismic design of new structures. These codes (and analogous normative documents in national contexts) implicitly distinguish between the seismic hazard assessment at regional scale (the 'reference' seismic hazard) and at 'local' level: the first is assessed by considering seismogenic processes and regional scale radiation pattern of earthquakes, the second by accounting for modification induced on the ground shacking at small scale (tens to hundreds of meters) geological-geomorphological settings.
These modifications are generally estimated by numerical modelling which accounts for the seismostratigraphical and geotechnical configuration of the local subsoil (e.g., Kramer, 1996). A key

element of this procedure is the definition of reference soil condition ('seismic' or 'engineering' bedrock), where the input seismic motion considered in the modelling is assumed to be known (e.g., by regional scale seismic hazard assessment). The parameterization of these models (in terms of Vs profiles, rigidity reduction and damping decay curves) must be performed by borehole and/or surface geophysical measurements (mainly active and passive seismic prospecting, e.g., Foti et al., 2011; Caielli et al.,2020) and laboratory tests (as concerns nonlinear aspects of soil dynamics).

When single buildings are of concern, seismic characterization relates to relatively small portions of the subsoil (the so called 'seismic response studies') and the relevant expenses could be supported by the stakeholders. However, when dealing with areal estimates, this analysis must be performed at many sites, and this makes the study very expensive, and this may hamper a generalized application of such analyses where public funds actually available are relatively scarce.

To face this problem, the strategies developed under the denomination of "Seismic Microzonation" (SM) are devoted to seismic hazard assessment at the scale of settlement and surrounding land (typically municipality). SM requires a strongly multidisciplinary approach must be developed which takes advantage of a full interoperability between geological/geomorphological surveys, geophysical prospecting, numerical modelling, and geotechnical laboratory testing. This marked interdisciplinarity requires a coherent methodological workflow between geologists, geophysicists, geotechnical engineers and, ultimately, land planners.

In the last years, the Italian scientific community (coordinated within the Centre for Seismic Microzonation and Applications – https://www.centromicrozonazionesismica.it/en/ under the coordination of the Civil Protection Department) developed specific guidelines for SM studies (WSGM 2008; WGSMLA 2010; Various Authors 2011). The guidelines delineate a gradual approach by defining three levels of SM studies, each characterized by increasing engagement and costs (e.g., Albarello, 2017; Moscatelli et al., 2020) in front of improved resolution and completeness. The first level is basically a collection of available information concerning shallow subsurface (i.e., borehole-data, geological/geomorphological surveys, geotechnical data) (CTMS, 2018) to assess a Geological-Geomorphological model after reclassification of geological units into engineering geological units following their geotechnical properties (thereafter gt_units) (ASTM, 2017; Amanti et al., 2020). This model subdivides the study area in homogeneous parcels of land (Seismically Homogenous Microzones, SHM) each characterized by similar expected co-seismic phenomena. Despite of the inherently semi-qualitative character of the SM first level, its outcomes are of primary importance for the subsequent levels. In the second level SM, amplification effects induced by the local 1D stratigraphical configuration are quantified by adopting a simplified approach based on the use of suitable abacuses (Peruzzi et al., 2016; Albarello et al., 2017; Paolucci et al., 2020). This second level SM can be seen as the first operative basis for land and emergency planning, providing specific indications to local authorities as concerns management of preventive activities (e.g., Mori et al., 2020). The third level SM only concerns small areas where complex effects (induced landslides, liquefaction, etc.) are expected and where simplified approaches cannot be effectively applied (Caielli et al., 2020; Ciancimino et al., 2020; Pagliaroli et al., 2020).

In this paper, we propose an integrated methodological workflow for SM studies that highlights the importance and the effectiveness of a complex Engineering Geological Model as basic prerequisite for 1D modelling of amplification effects. Three main steps are delineated: a) the combination of geological/geomorphological analyses to develop an Engineering-Geological Model of the study area (EGM); b) an upgraded model (Engineering-Geological/Geophysical Model, EGGM) by considering data provided by geophysical targeted prospecting; c) the definition of a SHM map based on EGGM by the use of suitable computational tools and the evaluation of the coherence of 1D Amplification Factors against the complexity of the EGGM. The workflow is illustrated by a case study based on a number of villages in Central Italy damaged during a Seismic sequence occurred in Central Italy during 2016-17 and where an intense SM campaign was carried out to support reconstruction activities (Moscatelli et al., 2020).

2. METHODOLOGICAL OUTLINE

The proposed methodological workflow is based upon the following steps:

a) assessment of the Engineering-Geological Model (EGM, Fig. 1a): concerns the definition of the zones characterised by homogeneous lithostratigraphical and geomorphological settings, including the semi-quantitative definition of representative lithostratigraphical logs and their geometrical relationships; in this evaluation the definition of the thickness ranges of the lithostratigraphical layers is relevant for geometrical relationships. Moreover, the geological units are reclassified in terms of (gt_units), *sensu* ASTM (2017) and CTMS (2018);

b) from EGM to the Engineering-Geological/Geophysical Model (EGGM, Fig. 1b): on the basis of the EGM, quick and low-cost surface geophysical investigations are planned to better constrain the vertical and lateral stratigraphical setting of SHMs and provide lithostratigraphical layers with seismic parameters (mainly Vs) and define representative lithostratigraphical logs for each SHM;

c) from EGGM to SHM Map (Fig. 1c): the EGGM is used to attribute Amplification Factor (AF) values to each SHM. Amplification factors are expressed in the form

$$AF_{T_1-T_2} = \frac{\int_{T_1}^{T_2} Sa_0 dT}{\int_{T_1}^{T_2} Sa_i dT} \quad ,[1]$$

where Sa_i e Sa_0 are the acceleration response spectra at the reference soil configuration and at the surface respectively. T_1 and T_2 are the extrema of range of building resonance periods of concern. In the Italian practice, three ranges are considered (0.1-0.5 s, 0.4-0.8 s, 0.7-1.1 s) representative of small, intermediate, and tall buildings (or seismically isolated) buildings. The respective values are determined from a small set of experimental proxies by using specific seismic abacuses representative of 1D resonance phenomena (WSGM, 2008). Eventually, presence of significantly different Amplification Factors within the same SHM may suggest its further subdivision by identifying new SHMs. The results are shown in a Map.

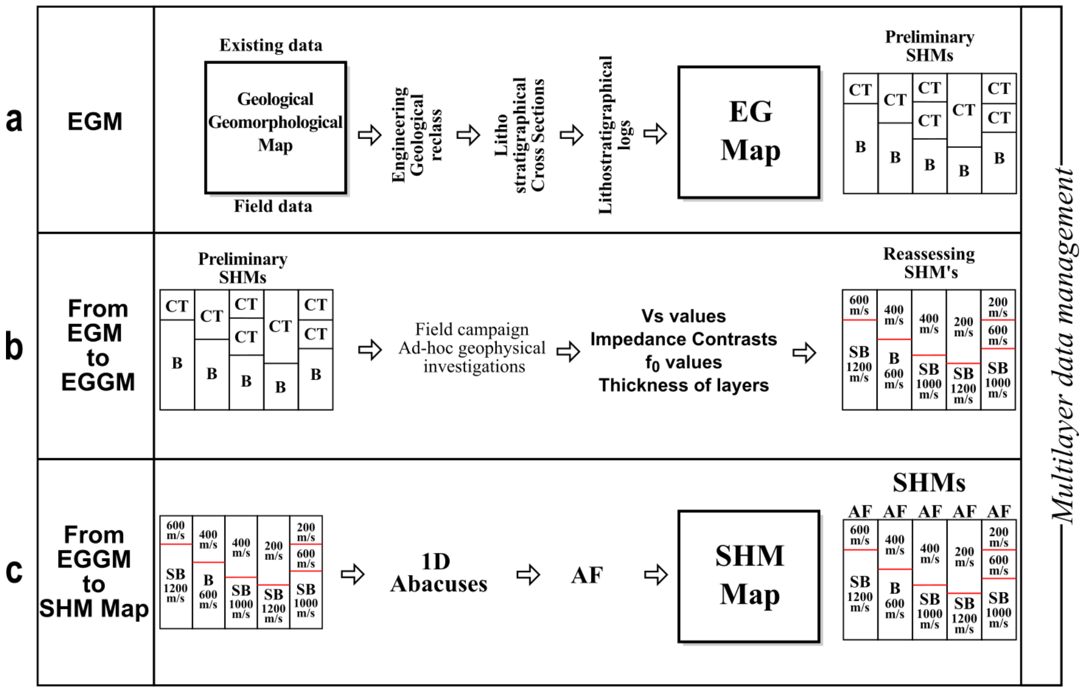

Fig. 1. Scheme of the methodological workflow. EGM, Engineering-Geological Model; EG Map, Engineering-Geological Map; CT, Cover Terrains; B, Bedrock; EGGM, Engineering-Geological/Geophysical Model; SB, Seismic Bedrock; SHM, Seismically Homogenous Microzone; AF, Amplification Factor (eq. 1); red lines within the SHM lithostratigraphical logs represent the position of the seismic impedance contrasts.

2.1 Assessment of EGM

EGM is a three-dimensional reconstruction of the lithostratigraphical sequences reclassified as gt_units and their volumetric distribution, including unstable areas (gravity phenomena, surface faulting, liquefaction and differential soil failures). EGM is represented by a map made of polygons classified as Bedrock and Cover Terrains (CT). Bedrock can be defined as the outcropping complex geological units/formations (sedimentary, magmatic, metamorphic) or unconformably buried under CTs. The last are made by units/formations related to the modelling of the present-day landscape and relative surface processes. In the geological-geomorphological setting of the Italian peninsula CTs are usually of Quaternary age whereas Bedrock is pre-Quaternary. CT are usually complex sedimentary bodies associated to morphogenetic processes (running water, gravity, karst, weathering, ice etc.) and therefore with extremely variable lateral extension and thickness. This variability is due to the presence of buried morphologies carved on Bedrock and to frequent and abrupt changes of facies associated to the different sedimentary environments and therefore showing a strong variability of geotechnical/geophysical properties. In terms of seismic behaviour, the sharper impedance contrast responsible for the main possible resonance phenomena is expected at the boundary between CTs and Bedrock, the latter represented by more rigid material. The high CT thickness variability can therefore cause the presence of impedance contrasts located at significantly different depths over distances of the order of hundreds of meters: it follows that, in the context of small-scale seismic hazard assessment, detailed geological and surveys are mandatory. In this framework, we assumed that thickness of the geological bodies in the EGM can be roughly classified as thin (3-10m), intermediate (10-100m) and thick (>100m).

EGM is at the base of any small-scale seismic hazard investigation and can be assessed only by expert-based observations, analysis and synthesis of existing data integrated with field data of new acquisitions. Existing data should be filtered according to their importance for EGM definition, such as local lithostratigraphical and structural settings, number and thickness of geological layers, geomorphological features and processes and, where available, geophysical and geotechnical parameters. Such data are usually gathered from National and Local databases and can consists of geological and geomorphological maps, local investigations such as cores, seismic surveys etc. The analysis of existing data is crucial to plan any further investigation.

In this first step, new field data are usually acquired by means of ex-novo geological and geomorphological surveys aimed at a more accurate definition of Bedrock and CT. To this purpose, the adopted legends should be based mainly on lithostratigraphical and morphogenetical criteria. Existing data and new field data integration lead to the first output that is a traditional Geological-Geomorphological Map reclassified and translated into an Engineering-Geological Map (Fig. 2a,b). The dimension of the subsurface volume to be assessed for EGM depends on the wavelength of seismic waves responsible for the damage of the structures. By assuming that these shear waves velocities in the shallow subsoil these are in the order of 200-600 m/s, for most common buildings with natural period of the order of 1s or less (IAEA, 2016) the wavelengths of the order of tens to hundreds of meters are of main importance. Therefore, the depth of subsoil to be characterized can be assumed at 150m for most of the situations. By the modelling of lithostratigraphical cross-sections (Fig. 2c) it is possible to identify the occurrence of different lithostratigraphical settings or logs, expressed by the number of stacked layers each represented in terms of: a) their belonging to the Bedrock or CT, b) type of gt_units according to conventional classification (e.g., ASTM, 2017), c) thickness range (Fig. 2d). Therefore, the EGM is a Map where any polygon corresponds to a preliminary SHM, characterised by the same subsurface lithostratigraphical setting and differs from a Geological-Geomorphological Map where only the surface geology is represented (Fig. 2e). It is worth to note that the thickness range includes the lateral variability expected in the microzone and the experimental uncertainty affecting thickness values assessed (or guessed) in this phase. In principle, the acquisition of more detailed information (i.e., by geophysical surveys) in the subsequent step does not necessarily imply a reduction of these ranges since the new data may reduce uncertainty but confirm or also increase the amount of expected lateral variability within the SHM.

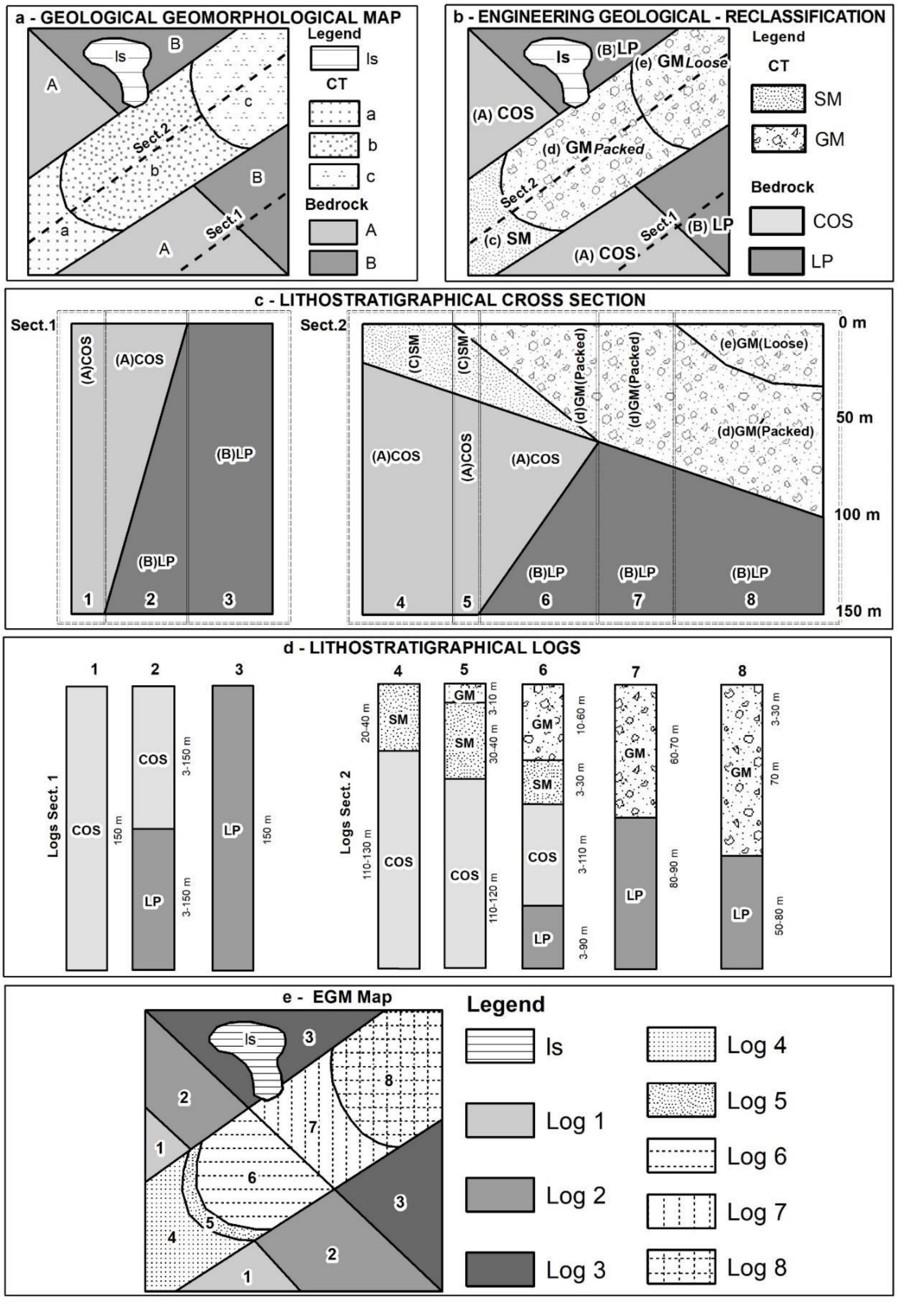

Fig. 2. Description of the EGM assessment methodology. a) Hypothetical CT (a-b-c) and Bedrock (A-B) units as mapped on a Geological-Geomorphological Map. Dashed lines represent the traces of the lithostratigraphical cross-sections. b) Engineering Geological reclassification of CT and Bedrock units: i.e., SM, Silty sands, mixed sands and silts; GM, Silty gravels, mixed gravels, sands and silts; COS, cohesive overconsolidated; LP, lapideous; ls, landslides. Dashed lines represent the traces of the lithostratigraphical cross-sections. c) Lithostratigraphical cross-sections according to gt_unit classification. d) Lithostratigraphical logs for each lithostratigraphical setting according to the section and thickness

variability for each layer. e) Engineering-Geological Model (EGM), the numbering of the mapped zones (which represent the preliminary SHMs) corresponds to the numbering of the lithostratigraphical logs.

2.2 From EGM to Engineering-Geological/Geophysical Model (EGGM)

In this phase, the aims are twofold. First, new field data corresponding to surface geophysical prospecting are carried out in order to provide further constraints to the geometries of lithological bodies delineated in the EGM. Second, these measurements will provide the seismic characterization of lithostratigraphic units present in the subsoil. Two main elements will be of main interest: a) the range of ground motion frequencies potentially affected by amplification effects (the 'resonance frequencies', f_0), b) Vs values representative of each lithostratigraphic unit identified in the EGM. The identification of main seismic impedance contrasts and of the identification of the Seismic Bedrock (SB) will also be of main concern. All these elements play a major role in assessing the local seismic hazard. SB represents the bottom of the seismo-stratigraphic log responsible for expected ground motion amplification.

The SB may or may not correspond to the Bedrock, depending on its characteristic Vs values. In fact, for engineering purposes, SB is conventionally defined with Vs values above any threshold (> 800 m/s in Italy by following the Italian Seismic Code NTC, 2018). This definition implies that, depending upon the geological characteristics and history, not all bedrocks are seismic bedrocks and eventually also CTs can be SB (i.e., hardly cemented or packed horizons within soft alluvial sediments). This phase allows the reassessment of representative lithostratigraphical logs for each polygon of the EGM Map, where the vertical sequence of gt_units is delineated with more refined thickness estimate (integrating geological and geophysical observations) along with respective Vs values (Fig. 1c).

Among many other seismic methods, recent practice in Italy (Albarello et al., 2015; Caielli et al., 2020) suggests that the ones based on surface waves prospecting procedures (e.g., Foti et al., 2011; Foti et al., 2017) played a major role in SM studies due to their cost-effectiveness, penetration depth, applicability in urban contexts. Both active and passive procedures based on single station (Bard, 1999) and array configurations (Okada, 2003; Park, 2011) have been largely used on purpose. A basic limitation of this approach relies on the strictly 1D interpretation of observations coupled with the strong non-linearity of the inversion procedure that only allows to define a range of Vs profiles compatible with observations. This ambiguity cannot be solved by considering the only geophysical methods but a strong integration of outcomes with geological interpretations is needed for a single comprehensive model of the subsoil. Anyway, relatively significant uncertainty margins will remain, which must be accounted for in subsequent analyses.

2.3 From EGGM to SHMs Map

The collected data allow to identify homogeneous areas roughly characterized by the same litho- and seismo-stratigraphical logs. These are: a) outcropping SB with expected AF = 1; b) areas where ground motion amplification is expected; c) unstable areas (landslides, capable faults, liquefaction).

This methodological step leads to a SM where only stable areas with 1D expected ground motion amplification are considered for the estimation of AF (eq. 1) that is calculated by suitable tools (abacuses) in the assumption that (e.g., Paolucci et al., 2020). The possible presence of more complex effects induced by the local complex geomorphological setting (abrupt slope changes, steep slopes, narrow ridges, peaks etc..) are also separately parameterized by considering specific abacuses (e.g., Ashford and Sitar, 1997; Paolucci, 2002) in the assumption that SB outcrops. Thus, two AFs are obtained respectively for lithostratigraphical and morphological effects and compared. When

morphological AF is comparable or larger than the lithostratigraphical one, a warning is associated to the relevant site by suggesting more advanced studies.
The output of this step is an SHM Map where each polygon is nearly homogeneous in terms of AF: a) if the same SHM shows a small variability of Amplification Factors (in the range of +/- 0.3, to say) the geometry of the SHM is confirmed and the relevant log is considered as representative of the whole SHM; b) where the same SHM shows a relatively large variability of AF then the spatial geometry of the SHM can change accordingly, i.e., by splitting SHM in more polygons; c) when two contiguous SHMs show similar AF they can be merged except when the geotechnical properties and parameters are significantly different.
To reach this goal the data collected during the workflow is continuously stored in a spatial database managed in Geographic Information System (GIS). To this purpose, a database structure has been developed in Italy by the Institute of Environmental Geology and Geoengineering of the National Research Council (CNR-IGAG) on behalf of the Italian Department for Civil Protection of the Presidency of Council of Ministers, to store information collected during seismic microzonation studies by following standardized procedures (DB SM, 2019).

3. CASE STUDY

3.1 Geographic, Geological and Geomorphological background

The study area is located in the Umbro-Marchean Apennine (Central Italy, Marche Region; Fig. 3a), an east-north-east verging fold-and-thrust belt developed due to the collision between the African and European plates (Boccaletti et al. 1990; Cavazza et al. 2004; Cosentino et al. 2010 and bibliography therein). The geological and geomorphological setting is the result of the complex interaction between the Meso-Cenozoic stratigraphy and structural evolution and the Quaternary tectonic uplift that led to the modelling of the present-day landscape (Calamita et al., 1999; Coltorti and Pieruccini, 1999).
Therefore, different morphostructural domains can be recognised at regional scale (Fig. 3a,b). They are characterised by distinctive geological and structural settings, peculiar morphological features and by different types of Bedrock and CTs (Amanti et al.,2020) described in the follows.
Mountain Ridges are characterised by elevations exceeding 2000 m a.s.l. and with steep to very steep slopes modelled on Bedrocks made of mainly calcareous Triassic-Oligocene formations belonging to the Umbro-Marchean succession (Centamore et al., 1986). Also, Mountain Ridges are bounded to the north-east by Miocene overthrusts (Fig. 3b) (Calamita and Deiana, 1988) and therefore the Bedrock is here commonly strongly fractured and weathered. The geomorphological processes associated to the landscape modelling led to the incision of deep valleys and to the deposition of shallow to thick CTs made of mostly coarse-grained alluvial and slope sediments.
Pedemountains Hills, characterized by gentle to steep slopes and elevations up to 1000 m a.s.l., are located to the NE and the SW of the MRs; the Bedrock is mainly made of alternating Oligocene-Miocene marls and limestones (Centamore et al., 1986) disturbed by the presence of overthrusts systems. CTs are dominated by coarse-grained alluvial and slope deposits and the valleys are wider than in Mountain Ridges and the slopes are affected by frequent gravity phenomena.
Terrigenous Hills, with elevations generally lower than 800 m a.s.l., have gentler slopes than Mountain Ridges and Pedemountains Hills and the Bedrock is mostly made of Messinian sandstones and clays belonging to foredeep siliciclastic turbiditic basins (Centamore et al., 1991) usually folded and faulted with local associated fracturing. CTs are mainly made of finer-grained slope and colluvial sediments and by coarse- to fine-grained alluvial deposits forming fluvial terraces within wide valley systems.

Periadriatic Hills, with elevations progressively decreasing toward the Adriatic coastline, are characterised by gentle slopes modelled on a Bedrock made of Pliocene-Lower Pleistocene marine clays and sands of the Periadriatic Basin (Bigi et al. 1997), deformed by gentler folds and only minor faults. CTs are fine-grained slope and colluvial deposits and coarse- to fine-grained alluvial sediments forming fluvial terraces within valleys that become progressively wider toward the coast.

The overall setting indicates the progressive change of engineering geological characteristics of Bedrocks from mainly lapideous (Mountain Ridges), to alternated lithologies (Pedemountain Hills), to granular (Terrigenous Hills) to overconsolidated cohesive and granular (Periadriatic Hills). Also, CTs characteristics change according to the distribution of the Bedrocks.

The case study are settlements located within Pedemountain Hills and Terrigenous Hills (respectively case study A and B in Fig. 3c) domains in the so-called Camerino Basin characterised by a strong historical seismic activity culminated with the 2016-2017 seismic sequence and associated damages (Galli et al., 2017). These localities are representatives of the geological-geomorphological contexts and settlement systems typical of the Northern Apennine where small historical villages are scattered in the landscape according to favourable topographic, land-use and climatic conditions.

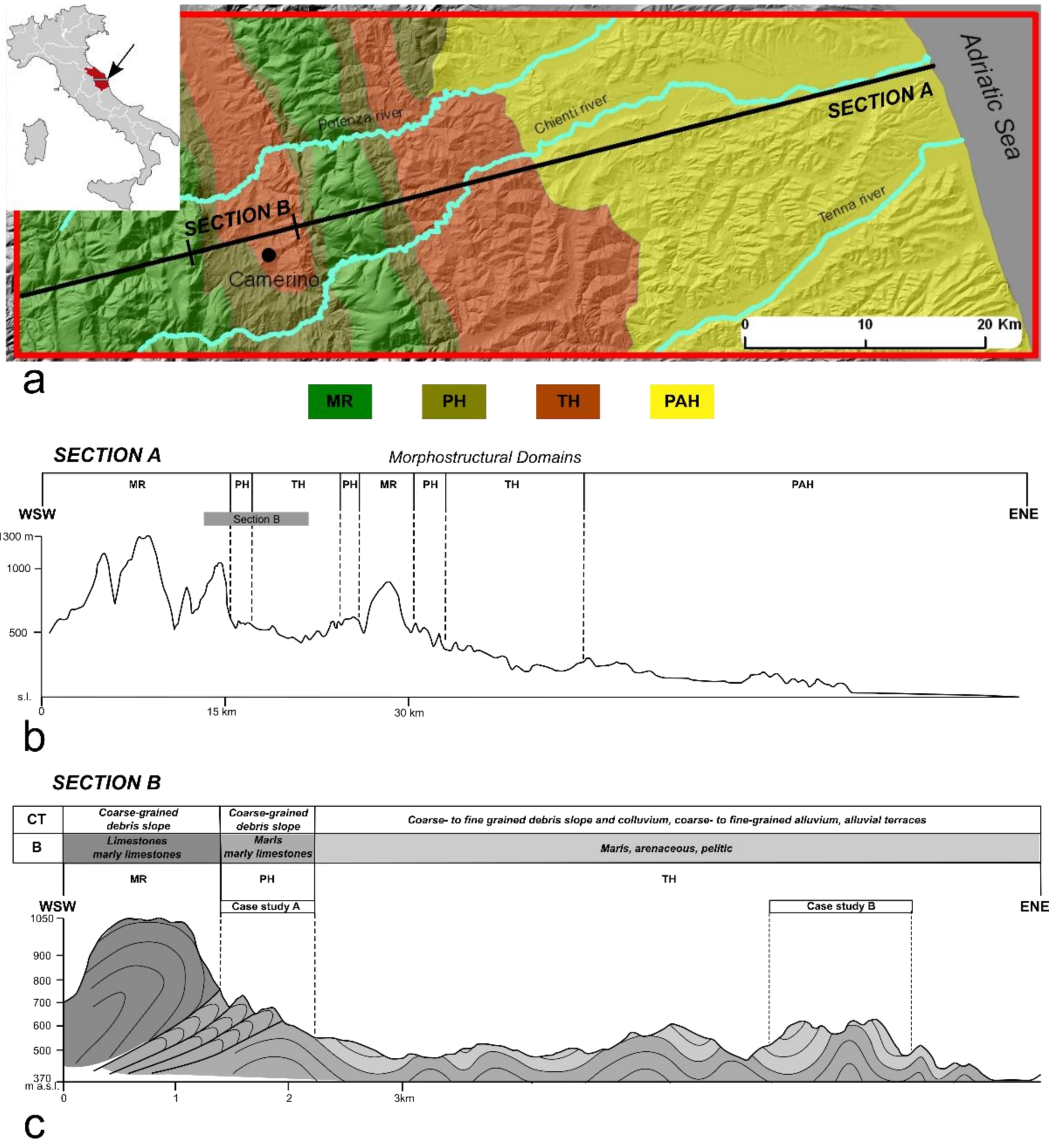

Fig. 3. a) The Morphostructural domains of the Umbro-Marchean Apennine (from Amanti et al., 2020 modified). MR – Mountain Ridges; PH – Pedemountain Hills; TH – Terrigenous Hills; PAH – Periadriatic Hills. b) Topographic section (section A) across the area with the indication of the Morphostructural domains. c) Simplified geological section across

the study area (section B) with the indication of the Morphostructural domains and the main types of Cover Terrains (CT) and Bedrock (B). The location of case studies is also reported.

3.2 The Engineering-Geological Model (EGM)

The EGM is assessed for the surrounding of the settlements following a Geological-Geomorphological analysis of a wider context for each morphostructural domain under study. The geological units (formal and informal lithostratigraphical units) are then reclassified and coded following their main engineering geological properties in terms of gt_units (Table 1).

	Geological Unit	Description	gt_code	gt_unit description
CT	Eluvial-colluvial deposits (Holocene)	Unsorted, loose to packed, mostly fine-grained deposits	**ML**	Inorganic silts, fine silty-clayey sands, low plasticity clayey silts
	Debris-slope deposits (Holocene)	Unsorted, loose to packed, angular to subangular, calcareous debris	**GP**	Not sorted gravels, mixed gravels and sands
	Debris-slope deposits (Late Pleistocene)	Unsorted, weakly to strongly cemented, angular to subangular calcareous debris	**GP**	Not sorted gravels, mixed gravels and sands
	Alluvial deposits (Late Pleistocene)	Unsorted, packed, subangular to rounded alluvial gravels and sands	**GM**	Silty gravels, mixed gravels, sands and silts
B	Camerino Formation FCIi	Pelitic-arenaceous lithofacies	**COS**	cohesive overconsolidated
	Camerino Formation FCId	Arenaceous lithofacies	**GRS**	grainy cemented stratified
	Schlier Formation SCH	Marls and clays	**COS**	cohesive overconsolidated
	Bisciaro Formation BIS	Marly limestones, marls and limestones	**ALS**	alternations of contrasting lithotypes
	Scaglia Cinerea Formation SCC	Limestones and marls	**ALS**	alternations of contrasting lithotypes

Table 1. Engineering geological reclassification of the Geological units in the study area: CT, Cover Terrains; B, Bedrock.

3.2.1 EGM Pedemountain Hills: S.Erasmo-Calcina-Arnano (case study A)

The area is characterised by the presence of 3 small settlements aligned at the north-eastern foot slopes of a Mountain Ridge reaching 1500 m asl in elevation (Fig. 3c). EGM is described for the immediate surroundings of the settlements and based on the Geological-Geomorphological map made by integrating existing data and ad hoc field surveys, lithostratigraphical cross sections (Fig. 4) and lithostratigraphical logs (Fig. 5) representative of the preliminary SHMs. In this step, gt_unit thickness ranges are preliminary assessed. The main structural feature is the presence of a series of thrusts affecting the Bedrock made of the uppermost marly-calcareous and marly-clayey formations of the Umbro-Marchean succession (Fig. 3c). The slopes are from medium to very steep, and characterised by two main generations of coarse-grained CTs, packed and locally cemented (Late Pleistocene) or poorly packed to loose (Holocene). Only in Calcina (Fig. 4 and Fig. 5) the two generations of debris slope deposits are superimposed. In S.Erasmo (Fig. 4 and Fig. 5) CTs are also made of a thin layer of poorly sorted, loose sandy-silty colluvial sediments related to the weathering of the marly-clayey Bedrock. The basal contact between CTs and the Bedrock is undulated or planar. The slopes are also affected by large- to medium-sized complex gravity phenomena.

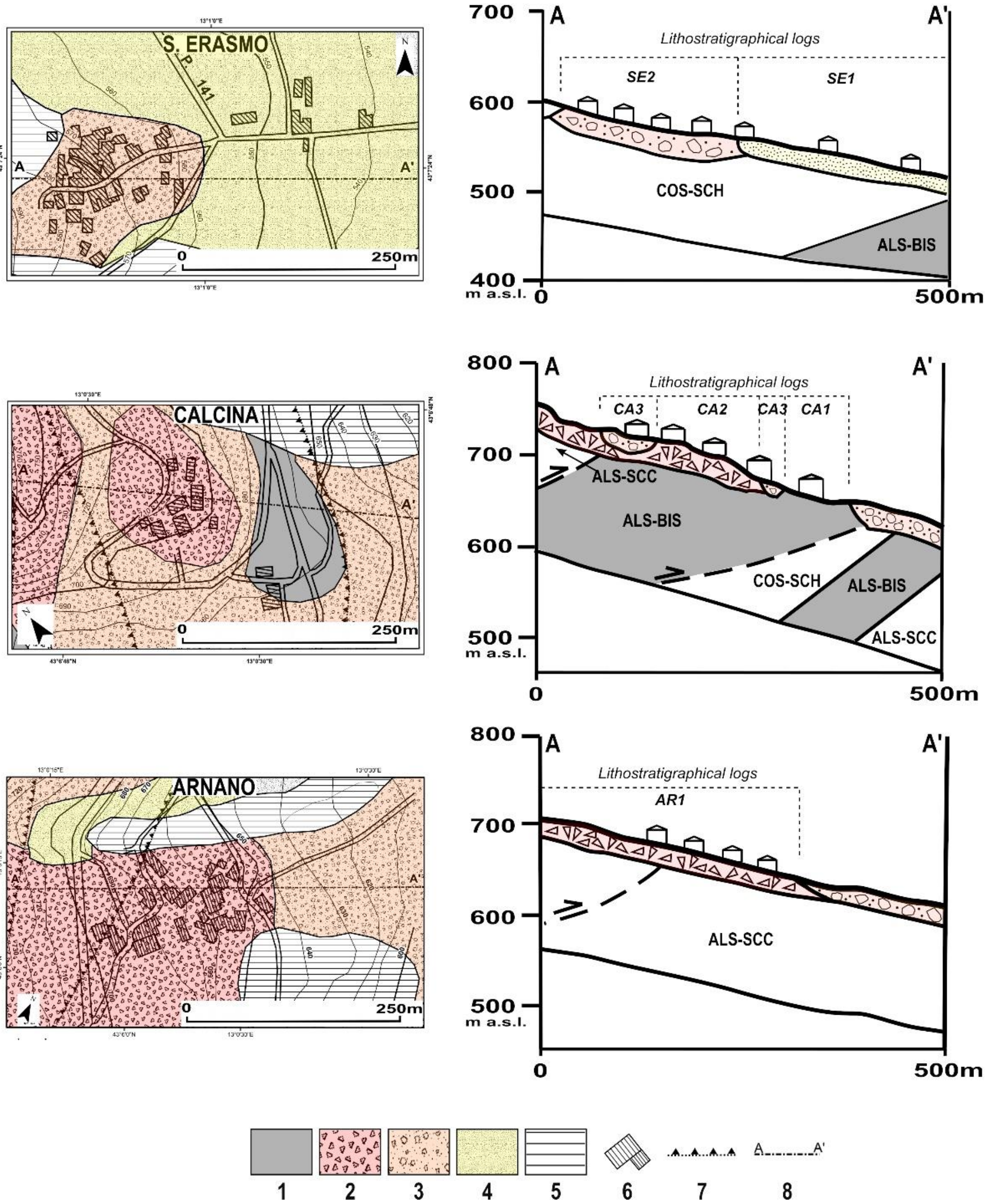

Fig. 4. Case study A, Engineering Geological Maps (left) and lithostratigraphical cross-sections (right) with correspondence to the lithostratigraphical logs of Fig. 5. For the engineering technical classification of gt_units see Table 1). Legend: 1 – Bedrock ALS; 2 – CT GP; 3 – CT GP; 4 – CT ML; 5 - Landslides; 6 - Buildings; 7 – Buried overthrusts; 8 – Trace of geological section.

Site	log id	Min (m)	Max (m)	B/CT	gt code	Description
SE - S.ERASMO	1	2	5	CT	ML	Unsorted low plasticity silts, clays and sands
		30	140	B	COS	Marls and clays (SCH Fm)
		10	70	B	ALS	Marly limestones (BIS Fm)
	2	5	25	CT	GP	Angular to subangular unsorted calcareous debris-slope, weakly to strongly cemented
				B	COS	Marls and clays (SCH Fm)
AR - ARNANO	1	5	20	CT	GP	Angular to subangular unsorted calcareous debris-slope, weakly to strongly cemented
				B	ALS	Limestones and marls (SCC Fm)
CA - CALCINA	1	70	100	B	ALS	Marly limestones (BIS Fm)
		10	20		COS	Marls and clays (SCH Fm)
		5	30		ALS	Marly limestones (BIS Fm)
	2	5	25	CT	GP	Angular to subangular unsorted calcareous debris-slope, weakly to strongly cemented
				B	ALS	Marly limestones (BIS Fm)
	3	5	15	CT	GP	Angular to subangular, loose, unsorted calcareous debris
		5	25	CT	GP	Angular to subangular unsorted calcareous debris-slope, weakly to strongly cemented
				B	ALS	Marly limestones (BIS Fm)

Fig. 5. Lithostratigraphical logs in S.Erasmo, Arnano and Calcina (Fig. 4). B: Bedrock; CT: Cover Terrains; gt_units: engineering technical classification (see Table 1); SCH, Schlier Fm; BIS Bisciaro Fm; SCC, Scaglia Cinerea Fm. The columns "Min" and "Max" identify the thickness ranges preliminarily associated to the geological units.

3.2.2 EGM Terrigenous Hills: S.Marcello-Sentino (case study B)

The area (Fig. 3c) is characterised by the presence of small settlements distributed on 3 different geomorphological setting: S.Marcello is located on a wide saddle at the head of a valley, Sentino and S.Silvestro over a hilltop (Fig. 6). The folded Bedrock is made of the Late Miocene marly-clayey and terrigenous rocks belonging to the Umbro-Marchean succession and Camerino Basin (SCH and FCI Fms). The slopes are gently steep to very steep, locally with stepped profiles due to selective erosion on the more resistant arenaceous Bedrock and the marly-clayey slopes are affected by shallow landslides. In S.Marcello, the wide saddle forms a wind gap belonging to a palaeo-drainage as confirmed by the presence of an alluvial gravelly horizon buried under recent colluvial deposits on the south-western slope (Fig. 6). In Sentino and S.Silvestro, CTs are very shallow (less than 2 m) or lacking on the steep slopes surrounding the settlements, mostly due to erosional runoff processes and anthropic activities (Fig. 6).

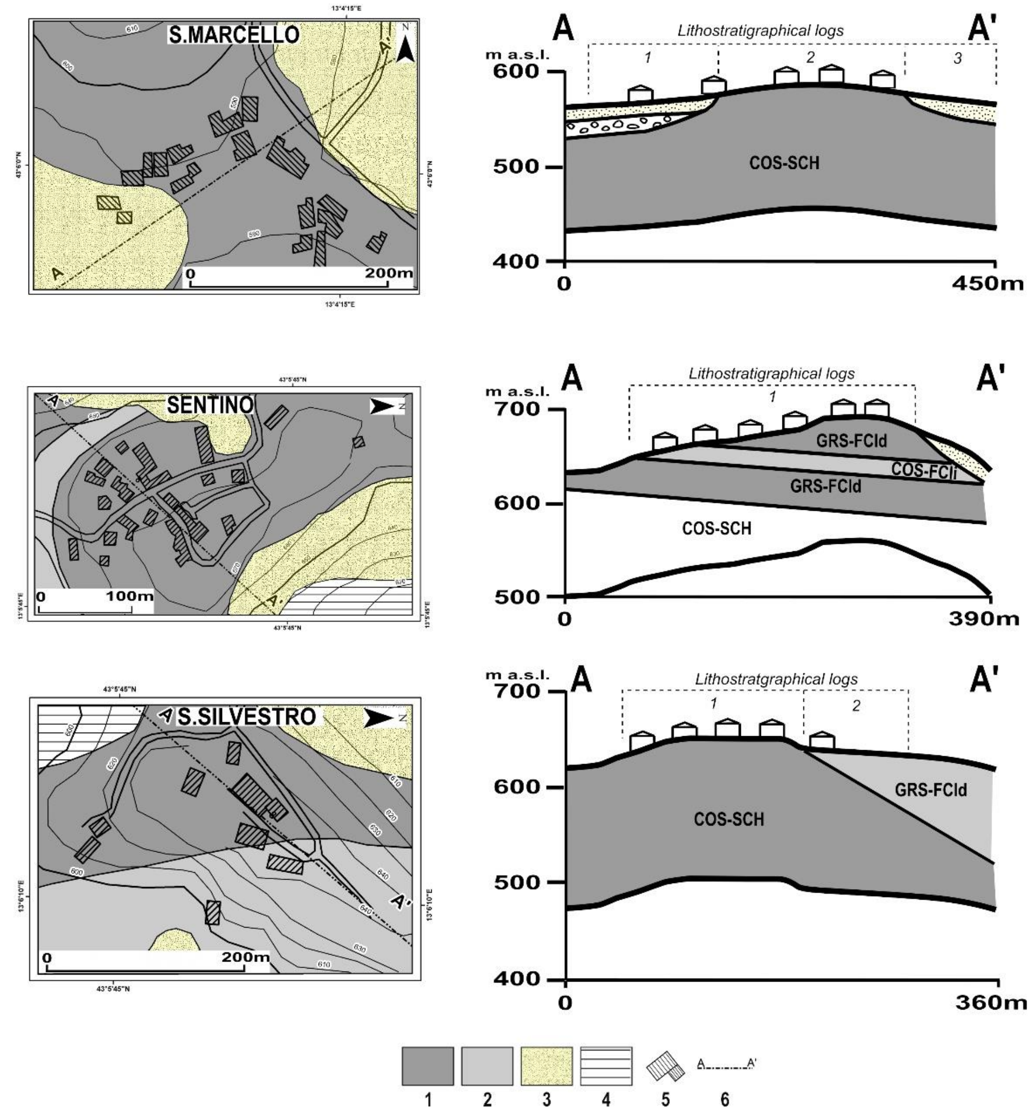

Fig. 6. Case study B, Engineering Geological Maps and lithostratigraphical cross-sections with correspondence to the lithostratigraphical logs of Fig. 7. Legend: 1 – Bedrock COS; 2 – Bedrock GRS; 3 – CT: ML; 4 - Landslides; 5 - Buildings; 6 – Trace of geological section.

SM - S.MARCELLO

log id	Min (m)	Max (m)	B/CT	gt code	Description
1	3	10	CT	ML	Holocene fine-grained unsorted eluvial and colluvial deposits
1	3	15	CT	GM	Pleistocene alluvial packed unsorted gravels and sands
1			B	COS	Marls and clays (SCH Fm)
2			B	COS	Marls and clays (SCH Fm)
3	3	10	CT	ML	Holocene fine-grained unsorted eluvial and colluvial deposits
3			B	COS	Marls and clays (SCH Fm)

SN - SENTINO

log id	Min (m)	Max (m)	B/CT	gt code	Description
1	3	50	B	GRS	Arenaceous lithofacies (FCId Fm)
1	15	15	B	COS	Pelitic-arenaceous lithofacies (FCIi Fm)
1	3	30	B	GRS	Arenaceous lithofacies (FCId Fm)
1			B	COS	Marls and clays (SCH Fm)

SS - S.SILVESTRO

log id	Min (m)	Max (m)	B/CT	gt code	Description
1			B	COS	Marls and clays (SCH Fm)
2	3	100	B	GRS	Arenaceous lithofacies (FCId Fm)
2			B	COS	Marls and clays (SCH Fm)

Fig. 7. Lithostratigraphical logs in S.Marcello, Sentino and S.Silvestro (Fig. 6). B: Bedrock; CT: Cover Terrains; gt_units: engineering technical classification (see Table 1); SCH, Schlier Fm; FCId, Camerino Fm; FCIi, Camerino Fm. The columns "Min" and "Max" identify the thickness ranges preliminarily associated to the geological units.

3.3 From EGM to EGGM

Geophysical surveys have been carried out in the study area to support geological analysis and provide the seismic parameterization of the gt_units present in the study area. To this purpose, both active and passive seismic prospecting were performed. The siting of these measurements was optimized by considering the preliminary EGM described above. Both active and passive prospecting techniques have been considered. Several single station measurements of ambient vibrations (see, e.g., Bonnefoy-Claudet et al., 2006) were performed to identify soil resonance frequency f_0 by the HVSR technique (e.g., Lachet and Bard, 1994; Bard, 1999). Array measurements (both in active and passive configurations) have been also carried out to infer representative Vs profiles from Rayleigh waves dispersion curves. MASW and ESAC/FK/MSPAC procedures were respectively used when active and passive configurations where respectively considered to determine the Rayleigh wave dispersion curve (e.g., Okada, 2003; Park, 2011; Foti et al., 2017). The choice between the two approaches depended on the specific situation: when deeper soft sedimentary covers were expected, the passive array has been preferred to the active one because of its greater penetration depth. As a whole, 103 HVSR measurements and 22 array surveys (22 active and at 7 sites accompanied by passive acquisitions) have been carried out in the study area. To retrieve the Vs profiles, assess the depth of main seismic impedance contrasts and SB as well as attributing representative seismic parameters to the gt_units, outcomes of the HVSR and array measurements were jointly inverted by using Genetic Algorithm, Monte Carlo or Simulated Annealing inversion procedure (e.g., Arai and Tokimatsu, 2005; Albarello et al., 2011; Garcia-Jerez et al., 2016). In order to explore possible uncertainty in the final outcome, the inversion has been carried out a number of times by retrieving each time the best fitting solution (e.g., Albarello et al., 2017). In Fig. 8, an example of results provided by the inversion process is reported as concerns colluvial deposits in the S. Marcello site (Fig. 7). One can see that a sharp seismic impedance contrast is detected around 25 m of depth at the bottom of the colluvial cover and that the range of experimental uncertainty is quite small.

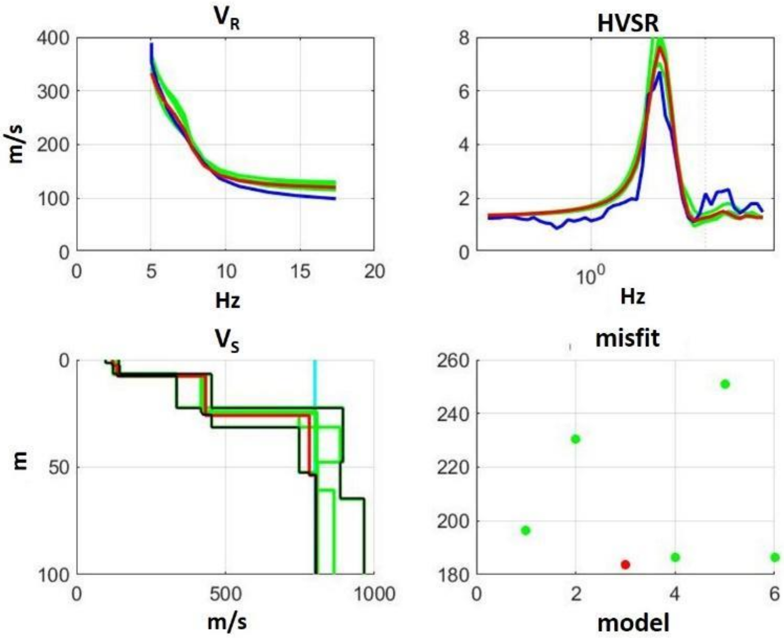

Fig. 8. Outcomes of the inversion of single station and array measurements at the S. Marcello site. In the figures at the top line, the experimental Rayleigh wave velocity (V_R) dispersion (top left) and HVSR (top right) curves are reported in blue. In these figures, theoretical curves provided by considering the models obtained by the inversion runs are reported in green. In red the overall best fitting solution is plotted. The corresponding misfit values are reported in the right figure at the bottom line. The Vs profiles corresponding to these runs are reported in right figure at the bottom. Black continuous lines indicate the confidence interval for the Vs values. The vertical light-blue line indicates the value corresponding to the conventional SB (800 m/s).

By considering outcomes of the geophysical survey, the gt_units present in the study area have been parameterized in terms representative thickness and Vs values (Fig. 9 and Fig. 10). In particular, in order to account for the expected lateral variations and experimental uncertainty, a range of possible values is attributed to both these parameters.

3.3.1 PH Pedemountain Hills

In most cases (Fig. 9) there is a good correspondence between the EGM and the observed geophysical parameters in terms of layer thicknesses. The total thickness range of the CT’s recognised in the EGM was over- or under-estimated but comparable with their expected lateral variability, ranging about 10-50% according to the availability or to the lack of suitable and reliable existing data. In Calcina 2 (Fig. 9), the CT layer was re-defined by 3 seismic layers according to the Vs value although within the same lithostratigraphical unit. Finally, an important contrast of impedance marks the boundary between CTs and the SB. In Calcina 2 and 3 (Fig. 9) the Bedrock (ALS-BIS Fm), buried under CTs, shows Vs values >800 m/s and therefore considered as SB. In Calcina 1 (Fig. 9) the outcropping Bedrock (ALS-BIS Fm) shows Vs values < 800 m/s and a progressive increase of velocity with depth, reaching values greater than 800 m/s at about 40 m and the impedance contrast is within the Bedrock.

This behaviour can be interpreted as due to the strong tectonic deformation related to the presence of thrust zones, typical of this morphostructural domain, with consequent strong physical and mechanical weathering of the outcropping Bedrock.
In the case of Arnano 1 and S.Erasmo 1 and 2 (Fig. 9), the Bedrock (respectively ALS-SCC Fm and COS-SCH Fm) shows the presence of Vs values increasing with depth, although with relatively high values (720-810 m/s) passing to higher values (> 1250 m/s) as in the case of Arnano 1.

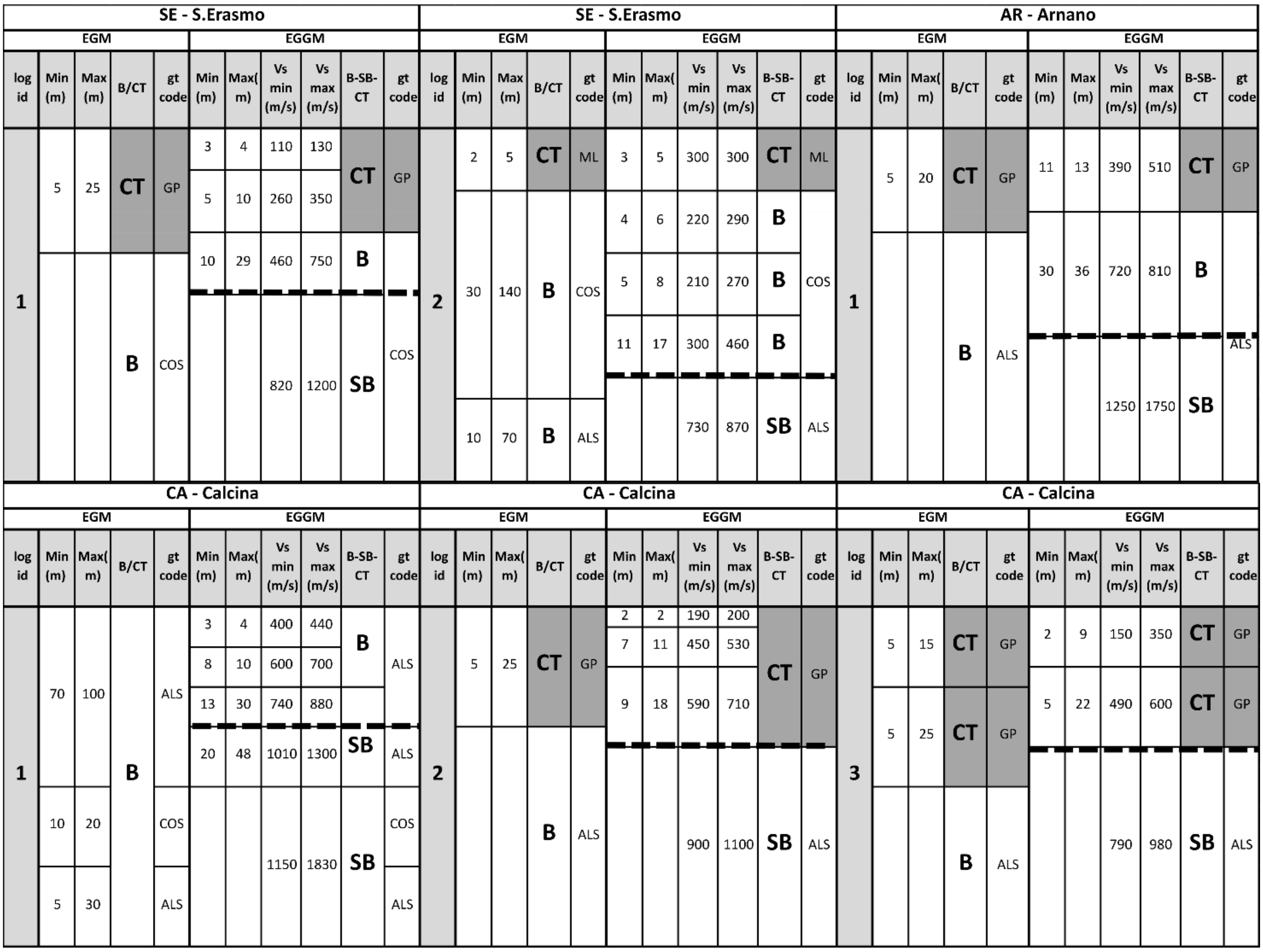

Fig. 9. Re-assessment of the S.Erasmo, Arnano and Calcina logs throughout the proposed methodological process, from EGM to EGGM. The dashed black lines are the main impedance contrasts detected for each litho-and seismo-stratigraphical logs characteristic for each SHM. B – Bedrock; SB – Seismic Bedrock; CT – Cover Terrains. For gt codes see Table 1.

3.3.2 TH Terrigenous Hills

At Sentino and S.Silvestro sites, runoff erosional processes reduced significantly the thickness of CTs along the slopes. Therefore, the geophysical investigations mostly pointed out to the seismic characteristics of the different types of Bedrocks.
At S.Silvestro 1 (Fig. 10), the outcropping Bedrock (COS-SCH Fm) revealed Vs values > 800 m/s. This is contrasting with the Vs values observed for the same Bedrock in the Pedemountain Hills morphostructural domain and can be explained with the different tectonic setting and the lack in Terrigenous Hills of thrust zones.
In Sentino 1 (Fig. 10), the alternances of pelitic-arenaceous and arenaceous lithofacies (ALS-FCI Fm), although well constrained in the EGM, are not evident after the geophysical investigations. The Vs values increase with depth and two important contrasts of impedance are present, the deepest one correlated to the boundary with the underlying Bedrock (COS-SCH Fm). Finally, at S.Silvestro 2

(Fig. 10) the Bedrock (GRS-FCI Fm) shows Vs values increasing with depth and the contrast of impedance is traced again at the boundary with the underlying Bedrock (COS-SCH Fm) also according to the observations made elsewhere in the same morphostructural domain. In S.Marcello (Fig. 10) there is a general very good correspondence between the EGM and the EGGM in terms of number of CTs layers and their thicknesses, also because EGM was well constrained due to the outcropping lithostratigraphical setting. The buried Bedrock (COS-SCH Fm) shows high Vs values, and the contrast of impedance is recorded between CTs and SB. In S.Marcello 2 (Fig. 10), the deeper layer of GM of S.Marcello 1 laterally disappear and the Bedrock become very close to the topographic surface turning thicker in S. Marcello 3 (Fig. 10). The EGM in this case was well constrained due to the presence of subsurface data and the EGGM substantially confirms the model.

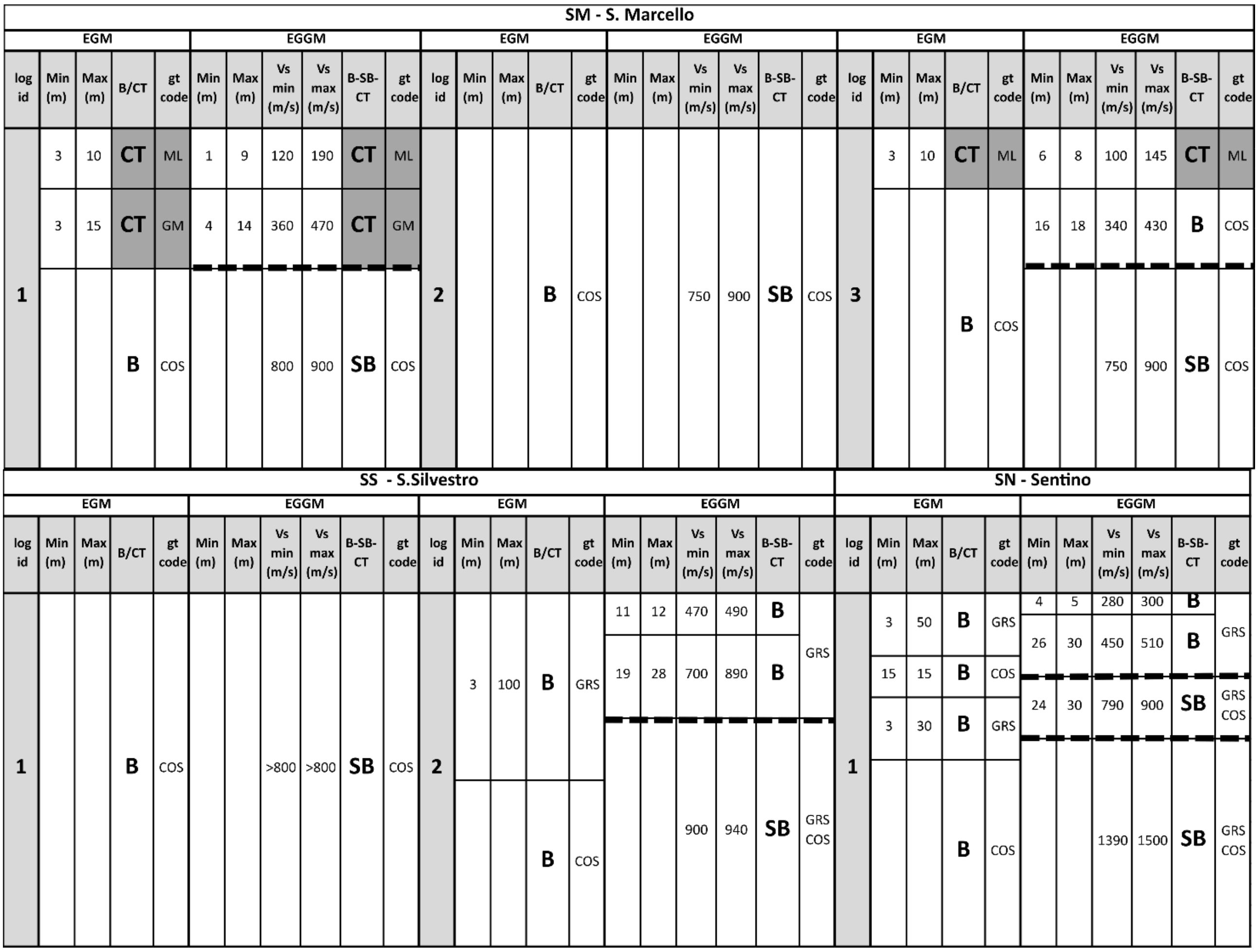

Fig. 10. Re-assessment of the S.Marcello, S.Silvestro and Sentino logs throughout the proposed methodological process, from EGM to EGGM. The dashed black line is the main impedance contrast. B – Bedrock; SB – Seismic Bedrock; CT – Cover Terrains. For gt_codes see Table 1.

3.4 Evaluating EGGM Map

The third step of the proposed approach aims at the quantification of expected amplification effects. To this purpose, standard numerical tools (e.g., Kottke and Rathje, 2008) are available. However, since the present study develops in the frame of seismic microzonation studies ruled by the Italian Guidelines for Seismic Microzonation, the quantification of stratigraphical amplification effects is here estimated by a simplified approach (Peruzzi et al., 2016). In particular, abacuses defined for Marche Region were considered to define values by assessing a small set of parameters. The abacuses to be used in the study area have been discussed in detail by Paolucci et al. (2020). By using this tool, three AFs are defined for each microzone relative to three ranges of building resonance periods (0.1-0.5s, 0.4-0.8s, 0.7-1.1s) by considering three pieces of information:

1. the geological domain (*sensu* Paolucci et al., 2020);
2. the SB depth;
3. the average Vs value to the SB (or to 30 m if the SB is deeper);
4. the fundamental soil resonance frequency f_0 estimated from HVSR measurements.

As one can see all the above parameters can be deduced from the EGGM. This also implies that several FA values could be obtained for the same microzone in the case that several f_0 measurements have been performed in that zone. Eventual significant differences among the FA values for the same microzone could suggest that lateral variations exist (eventually considered as negligible in the previous phases), which may result in significant differences in the local seismic hazard. This may suggest the splitting of the relevant microzone to identify new microzones more homogeneous in terms of relative hazard. If within the SHM no ground motion amplification is expected, i.e., where SB outcrops or where CTs or Bedrock are characterized by thicknesses lower than 3 m, the relevant AFs assume values equal to 1. In the case studies, the possible presence of morphological amplification effects has been evaluated and shown to be negligible.
By considering these elements, the relevant AF values have been computed for both case studies (Table 2). The final SHM Maps are reported in Fig. 11. Observing the AF values and Fig .9 and Fig. 10, it is possible to note that the highest ones (considering all the period ranges) are associated to the SHMs where the layers above the SB are characterized by the lowest Vs values. No significant differences appear to be related to the SB depth. S.Marcello 2 (SM 2) and S.Silvestro 1 (SS 1) are two SHMs where no ground motion amplification is expected. Moreover, no significant differences emerged between the estimate of AF values within the same SHM and thus it was not necessary to change geometry of the SHMs. Implicitly, thus outcome supports effectiveness of the EGGM model in the context of this case study.

SHM	AF 0.1-0.5 s	AF 0.4-0.8 s	AF 0.7-1.1 s
SE 1	2.2	2.5	2.3
SE 2	2.4	2.5	2.3
CA 1	1.5	1.5	1.3
CA 2	1.6	1.8	1.8
CA 3	2.6	1.8	1.5
AR 1	1.4	1.3	1.1
SM 1	2.5	2	1.4
SM 2	1	1	1
SM 3	2.4	2	1.4
SN 1	1.6	1.8	1.5
SS 1	1	1	1
SS 2	1.6	1.5	1.4

Table 2. AF values estimated using the abacuses for the SHMs belonging to the Pedemountain Hills considering the three period ranges. SE – S.Erasmo; CA – Calcina; AR – Arnano; SM – S.Marcello; SN – Sentino; SS – S.Silvestro.

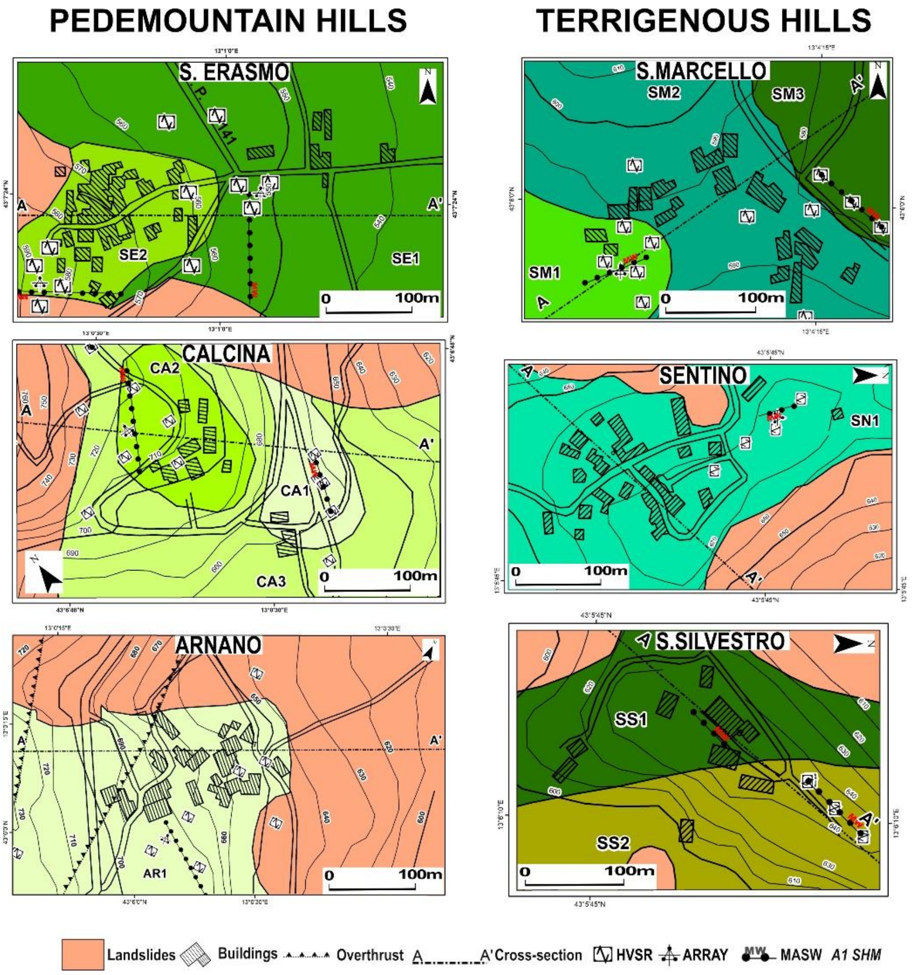

Fig. 11. SHM Maps of the case studies. The grey colours are referred to the SHMs described in Fig. 9, Fig. 10 and Table 2.

5. CONCLUSIONS

Several seismic microzonation procedures have been applied worldwide in the last years (e.g, Thitimakorn, 2019; Molnar et al., 2020; Régnier et al. 2020; Salsabili et al., 2021; Mase et al., 2021) by considering both geological and geophysical/geotechnical information to constrain expected amplification effects. In most cases, engineering geological information plays a minor qualitative role and no specific protocol is defined to standardize its implementation in microzonation studies. This last issue is the aim of the present contribution. In particular, a workflow has been delineated aiming at providing a methodological basis for a full integration of geological/geomorphological and geophysical protocols for the seismic characterization of wide areas (Seismic Microzonation). The first main goal of this methodological approach is obtaining maximum results by minimizing costs. This makes the proposed approach feasible also where economic resources are scarce (small settlements, developing countries, etc.). In this view, the assessment of a reliable Engineering-Geological Model (in the perspective of seismic response analysis) is of main importance to assess a three-dimensional distribution of lithostratigraphical settings, to orient geophysical surveys and to provide a coherent interpretative framework. The workflow here proposed includes three steps: a) the development of a 3D reference engineering geological model resulting in the partition of the study area into homogeneous microzones (in the perspective of hazard assessment), b) the refinement of this model by considering outcomes of on-purpose geophysical surveys and the seismic parameterization of the microzones, c) the preliminary quantification of expected amplification the phenomena in each microzone. The results show as the evaluated AF are consistent with the EGGM emphasizing the importance of a well-established model that *de facto* makes simpler the evaluation of seismic hazard. The results of this approach are of paramount importance for land planning and particularly in the framework of restoration policies. In fact, despite the approximate character of hazard estimates, outcomes will also allow the identification of areas where the expected enhancement of seismic ground motion may suggest detailed seismic response studies before planning new constructions. This approach to local seismic hazard assessment cannot be considered as alternative to site specific seismic response studies required by seismic regulations for anti seismic design of single buildings. Anyway, it may provide useful constraints for these studies. In particular, information provided by Seismic Microzonation may be useful to assess the dimension of the volume of subsoil (the "site domain" defined by IAEA, 2016) to be characterized in detail to provide effective numerical estimates of the local seismic response.

ACKNOWLEDGEMENTS

We are grateful to Silvia Marchese, Valerio Ferrazza and Michele Amaddii for their help in performing geophysical and geological/geomorphological surveys in the investigated areas. Vincenzo.Amato and the other anonymous referee also provided encouraging comments and suggestions to improve the paper. The work has bene developed in the frame of scientific activity of the Center for Seismic Microzonation and Applications (https://www.centromicrozonazionesismica.it/en/)

DECLARATIONS

Funding: Not applicable
Conflicts of interest/Competing interests: Not applicable
Availability of data and material: Not applicable
Code availability: Not applicable
Authors' contributions (optional: please review the submission guidelines from the journal whether statements are mandatory)

REFERENCES

Albarello, D., Cesi, C., Eulilli, V., Guerrini, F., Lunedei, E., Paolucci, E., Pileggi, D., Puzzilli, L.M., 2011. The contribution of the ambient vibration prospecting in seismic microzoning: an example from the area damaged by the 26th April 2009 L'Aquila (Italy) earthquake. Boll.Geofis.Teor.Appl. 52, 513-538. https ://doi.org/10.4430/bgta0013.

Albarello, D., Socco, L.V., Picozzi, M., Foti, S., 2015. Seismic Hazard and land management policies in Italy: the role of seismic investigations. First Break 33, 87-93. https://doi.org/10.3997/1365-2397.33.8.82009.

Albarello, D., Francescone, M., Lunedei, E., Paolucci, E., Papasidero, M.P., Peruzzi, G., Pieruccini, P., 2017. Seismic characterization and reconstruction of reference ground motion at accelerometric sites of the Italian national accelerometric network (RAN). Nat Hazards 86, 401-416. https://doi.org/10.1007/s11069-016-2310-4.

Albarello, D., 2017. Extensive application of seismic microzoning: methodological and socio-political issues in the Italian Experience. Boll.Geofis.Teor.Appl. 58, 4, 253-264. DOI 10.4430/bgta0205.

Amanti, M., Chiessi, V., Muraro, C., Puzzilli, L.M., Roma, M., Catalano, S., Romagnoli, G., Tortorici, G., Cavuoto, G., Albarello, D., Fantozzi, P.L., Paolucci, E., Pieruccini, P., Caprari, P., Mirabella, F., Della Seta, M., Esposito, C., Di Curzio, D., Francescone, M., Pizzi, A., Macerola, L., Nocentini, M., Tallini, M., 2020. Geological and geotechnical models definition for 3rd level seismic microzonation studies in Central Italy. Bull.Earthq.Eng. 18, 5441-5473. https://doi.org/10.1007/s10518-020-00843-x.

Arai, H., Tokimatsu, K., 2005. S-wave velocity profiling by joint inversion of microtremor dispersion curve and horizontal-to-vertical (H/V) spectrum. Bull. Seismol. Soc. Am. 95, 5, 1766-1778. https://doi.org/10.1785/0120040243**.**

Ashford, S.A., Sitar, N., 1997. Analysis of topographic amplification of inclined shear waves in a steep coastal bluff. Bull.Seismol.Soc.Am. 87, 692-700.

ASTM, 2017. Standard Practice for Classification of Soils for Engineering Purposes (Unified Soil Classification System), ASTM International, West Conshohocken, PA, www.astm.org.

Baratta, M., 1910. La catastrofe sismica calabro messinese : 28 dicembre 1908. Società geografica italiana, reprinted by Forni, 1985, Bologna (in Italian).

Bard, P.Y., 1999. Microtremor measurements: a tool for site effect estimation? In: Irikura, K., Kudo, K., Okada, H., Sasatani, T. (Eds.), The effects of surface geology on seismic motion. Balkema, Rotterdam, pp. 1251–1279. ISBN 90 5809 0302.

Bigi, S., Cantalamessa, G., Centamore, E., Didaskalou, P., Micarelli, A., Nisio, S., Pennesi, T., Potetti, M., 1997. The periadriatic basin (Marche-Abruzzi sector, Central Italy) during the Plio-Pleistocene. Giorn. Geol. 59, 245-259.

Boccaletti, M., Calamita, F., Deiana, G., Gelati, R., Massari, F., Moratti, G., Ricci Lucchi, F., 1990. Migrating foredeep-thrust belt system in the Northern Apennines and Southern Alps. Paleo. Paleo. Paleo 77, 3-14. https://doi.org/10.1016/0031-0182(90)90095-O.

Bonnefoy-Claudet, S., Cotton, F., Bard, P.Y., 2006. The nature of noise wavefield and its applications for site effects studies: a literature review. Earth. Sci. Rev. 9, 205-227. https://doi.org/10.1016/j.earscirev.2006.07.004.

BSSC NEHRP, 2000. Recommended Provisions for Seismic Regulations for New Buildings and Other Structures. 2000 Edition, Building Seismic Safety Council for the Federal Emergency Management Agency (FEMA Rep. 368, 369), Part 1: Provisions (FEMA Report 368); Part 2: Commentary (FEMA Report 369), Washington, D.C.

Caielli, G., De Franco, R., Di Fiore, V., Albarello, D., Catalano, S., Pergalani, F., Cavuoto, G., Cercato, M., Compagnoni, M., Facciorusso, J., Famiani, D., Ferri, F., Imposa, S., Martini, G., Paciello, A., Paolucci, E., Passeri, F., Piscitelli, S., Puzzilli, L.M., Vassallo, M., 2020. Extensive surface geophysical prospecting for seismic microzonation. Bull.Earthq.Eng. 18, 5475-5502. https://doi.org/10.1007/s10518-020-00866-4.

Calamita, F., Deiana, G., 1988. The arcuate shape of the Umbria-Marche-Sabina Apennines (Central Italy). Tectonophysics 146, 139–147. https://doi.org/10.1016/0040-1951(88)90087-X.

Calamita, F., Coltorti, M., Pieruccini, P., Pizzi, A., 1999. Evoluzione strutturale e morfogenesi plio-quaternaria dell'Appennino umbro-marchigiano tra il pedappennino umbro e la costa adriatica. Boll. Soc. Geol. It. 118, 125-139 (in Italian).

Cavazza, W., Roure, F., Ziegler, P.A., 2004. The Mediterranean area and the surrounding regions: active processes, remnants of former Tethyan oceans and related thrust belts, in: Cavazza, W., Roure, F., Spakman, W., Stampf, G.M., Ziegler, P.A. (Eds.), The TRANSMED Atlas. The Mediterranean Region from crust to mantle. Springer, Berlin, pp. 1–29.

Centamore, E., Deiana, G., Micarelli, A., Potetti, M., 1986. Il Trias-Paleogene delle Marche, in: Centamore, E., Deiana, G. (Eds.), La Geologia delle Marche. Studi Geol. Camerti, Volume Speciale, pp. 9-27 (in Italian).

Centamore, E., Cantalamessa, G., Micarelli, A., Potetti, M., Berti, D., Bigi, S., Morelli, C., Ridolfi, M., 1991. Stratigrafia ed analisi di facies dei depositi del Miocene e del Pliocene inferiore dell'avanfossa marchigiano-abruzzese e delle avanfosse limitrofe. Studi Geol. Camerti, Vol. Spec. 1991/2, 125-132 (in Italian).

Ciancimino, A., Lanzo, G., Alleanza, G.A., Amoroso, S., Bardotti, R., Biondi, G., Cascone, E., Castelli, F., Di Giulio, A., D'Onofrio, A., Foti, S., Lentini, V., Madiai, C., Vessia, G., 2020. Dynamic characterization of fine‐grained soils in Central Italy by laboratory testing. Bull.Earthq.Eng. 18, 5503-5531. https://doi.org/10.1007/s10518-019-00611-6.

Coltorti, M., Pieruccini, P., 1999. A late Lower Pliocene planation surface across the Italian Peninsula: a key tool in neotectonic studies. Journal of Geodynamics 29, 323-328. https://doi.org/10.1016/S0264-3707(99)00049-6.

Cosentino, D., Cipollari, P., Marsili, P., Scrocca, D., 2010. Geology of the central Apennines: a regional review, in: Beltrando, M., Peccerillo, A., Mattei, M., Conticelli, S., Doglioni, C. (Eds.), Journal of the Virtual Explorer, 36, paper 11. doi:10.3809/jvirtex.2009.00223.

CTMS (Commissione tecnica per la Microzonazione sismica), 2018. Standard di Rappresentazione ed archiviazione informatica, versione 4.1.1, Dept.of Civil Protection, Rome (in Italian), available on the website: https://www.centromicrozonazionesismica.it/it/download/send/26-standardms-41/71-standardms-4-1.

DB-SM. Portale cartografico della Microzonazione Sismica e della Condizione Limite per l'Emergenza, https://www.webms.it/servizi/viewer.php; 2019 [accessed, March 2020].

EN 1998-1, 2004. Eurocode 8: Design of structures for earthquake resistance. Part 1: General rules, seismic actions and rules for buildings, Brussels.

Faccioli, E. (Ed.), 1986. Elementi per una guida alle indagini di microzonazione sismica, Consiglio Nazione delle Ricerche, Rome (in Italian).

Foti, S., Parolai, S., Albarello, D., Picozzi, M., 2011. Application of surface wave methods for seismic site characterization. Surv.Geophys. 32, 6, 777-825. DOI 10.1007/s10712-011-9134-2.

Foti, S., Hollender, F., Garofalo, F., Albarello, D., Asten, M., Bard, P.Y., Comina, C., Cornou, C., Cox, B., Di Giulio, G., Forbriger, T., Hayashi, K., Lunedei, E., Martin, A., Mercerat, D., Ohrnberger, M., Poggi, V., Renalier, F., Sicilia, D., Socco, V., 2017. Guidelines for the good practice of surface wave analysis: a product of the InterPACIFIC project. Bull.Earthq.Eng. 16, 2367–2420. https://doi.org/10.1007/s10518-017-0206-7.

Galli, P., Castenetto, S., Peronace, E., 2017. The macroseismic intensity distribution of the 30 October 2016 earthquake in central Italy (Mw 6.6): seismotectonic implications. Tectonics 36, 2179-2191. https://doi.org/10.1002/2017TC004583.

García-Jerez, A., Piña-Flores, J., Sánchez-Sesma, F.J., Luzón, F., Perton, M., 2016. A computer code for forward computation and inversion of the H/V spectral ratio under the diffuse field assumption. Computers & Geosciences 97, 67-78. https://doi.org/10.1016/j.cageo.2016.06.016.

IAEA, 2016. Seismc hazard assessment in site evaluation for nuclear installations: ground motion prediction equations and site response, IAEA-TECDOC-1796, Wien.

Khan, S., Waseem, M., Khan, M.A., Hussain Z., Ahmed W., Khliq A.H., Umair N.S., Hissain M.L., 2020. Microzonation map of the Abbottabad basin and immediate surroundings. J Seismol 24, 165–181 (2020). https://doi.org/10.1007/s10950-019-09895-2

Kottke, A.R. and Rathje E.M.. 2008. "Technical manual for Strata." Report No.: 2008/10. Pacific Earthquake Engineering Research Center, University of California, Berkeley.

Kramer, S.L., 1996. Geotechnical Earthquake Engineering, Prentice Hall, New Jersey, USA.

Lachet, C., Bard, P.Y., 1994. Numerical and theoretical investigations on the possibilities and limitations of Nakamura's technique. J Geophys Earth 42, 377-397. https://doi.org/10.4294/jpe1952.42.377.

Mase, L.Z., Sugianto, N. & Refrizon, 2021. Seismic hazard microzonation of Bengkulu City, Indonesia. Geoenviron Disasters 8, 5. https://doi.org/10.1186/s40677-021-00178-yMedvedev, S.V., 1965. Engineering Seismology, Israel Program fo Scientific Translations Ltd., Jerusalem.

Molnar S., Assaf J., Sirohey A., Adhikari S.R., 2020. Overview of local site effects and seismic microzonation mapping in Metropolitan Vancouver, British Columbia, Canada, Eng. Geol., 270, 105568, https://doi.org/10.1016/j.enggeo.2020.105568.

Mori, F., Gaudiosi, I., Tarquini, E., Bramerini, F., Castenetto, S., Naso, G., Spina, D., 2020. HSM: a synthetic damage‑constrained seismic hazard parameter. Bull.Earthq.Eng. 18, 5631-5654. https://doi.org/10.1007/s10518-019-00677-2.

Moscatelli, M., Albarello, D., Scarascia Mugnozza, G., Dolce, M., 2020. The Italian approach to seismic microzonation. Bull.Earthq.Eng. 18, 5425–5440. https://doi.org/10.1007/s10518-020-00856-6.

NTC, 2018. Norme Tecniche per le Costruzioni. Decreto del Ministero delle Infrastrutture, GU serie generale n.42, 20-02-2018 – Suppl. Ordinario n.8

Okada, H., 2003. The microtremor survey method, Geophysical Monograph Series, 12, Society of Exploration Geophysicists. https://doi.org/10.1190/1.9781560801740.

Pagliaroli, A., Pergalani, F., Ciancimino, A., Chiaradonna, A., Compagnoni, M., De Silva, F., Foti, S., Giallini, S., Lanzo, G., Lombardi, F., Luzi, L., Macerola, L., Nocentini, M., Pizzi, A., Tallini, M., Teramo, C., 2020. Site response analyses for complex geological and morphological conditions: relevant case-histories from 3rd level seismic microzonation in Central Italy. Bull.Earthq.Eng. 18, 5741–5777. https://doi.org/10.1007/s10518-019-00610-7.

Paolucci, R., 2002. Amplification of earthquake ground motion by steep topographic irregularities. Earthquake Engineering and Structural Dynamics 31, 1831-1853. https://doi.org/10.1002/eqe.192.

Paolucci, E., Tanzini, A., Peruzzi, G., Albarello, D., Tiberi, P., 2020. Empirical testing of a simplified approach for the estimation of 1D lithostratigraphical amplification factor. Bull.Earthq.Eng. 18, 1285–1301. https://doi.org/10.1007/s10518-019-00772-4.

Park, C.B., 2011. Imaging dispersion of MASW data - full vs. selective offset scheme. Journal of Environmental and Engineering Geophysics 16, 1, 13-23. https://doi.org/10.2113/JEEG16.1.13.

Peruzzi, G., Albarello, D., Baglione, M., D'Intinosante, V., Fabbroni, P., Pileggi, D., 2016. Assessing 1D seismic response in microzoning studies in Italy. Bull.Earthq.Eng. 14, 373-389. https://doi.org/10.1007/s10518-015-9841-z.

Régnier J., Bertrand E., Cadet H., 2020. Repeatable process for seismic microzonation using 1-D site-specific response spectra assessment approaches. Application to the city of Nice, France, Eng. Geol., 270, 105569, https://doi.org/10.1016/j.enggeo.2020.105569.

Salsabili, M., Saeidi, A., Rouleau, A., Nastev N., , 2021. Seismic microzonation of a region with complex surficial geology based on different site classification approaches. Geoenviron. Disasters 8, 27 (2021). https://doi.org/10.1186/s40677-021-00198-8

Thitimakorn T., 2019. Seismic microzonation maps of Phrae city, Northern Thailand, Geomatics, Natural Hazards and Risk, 10:1, 2276-2290, DOI: 10.1080/19475705.2019.1693705

Various Authors, 2011. Contributi per l'aggiornamento degli ''Indirizzi e criteri per la microzonazione sismica'', in: Ingegneria Sismica, 28, 2, Patron editore, Bologna, Italy (in Italian), http://www.protezionecivile.gov.it/resources/cms/documents/aggiornamento_indirizzi_microzonazione_sismica.pdf.

WGSM (Working Group on Seismic Microzoning), 2008. Indirizzi e criteri per la microzonazione sismica, Conferenza delle Regioni e delle Province autonome – Dipartimento della Protezione Civile, Rome, 3 vol. and DVD (in Italian), http://www.protezionecivile.gov.it/jcms/it/view_pub.wp?conte ntId=PUB1137, English version at http://www.protezionecivile.gov.it/httpdocs/cms/attach_extra/GuidelinesForSeismicMicrozonation.pdf?.

WGSMLA (Working Group on Seismic Microzoning the L'Aquila Area), 2010. Microzonazione sismica per la ricostruzione dell'area aquilana, Regione Abruzzo, Dipartimento della Protezione Civile, 3 vols and DVD, 796 pp. (in Italian), http://www.protezionecivile.gov.it/jcms/it/view_pub.wp?conte ntId=PUB25 330.

Figure 1

Click here to access/download;Figure;FIG_1.jpg

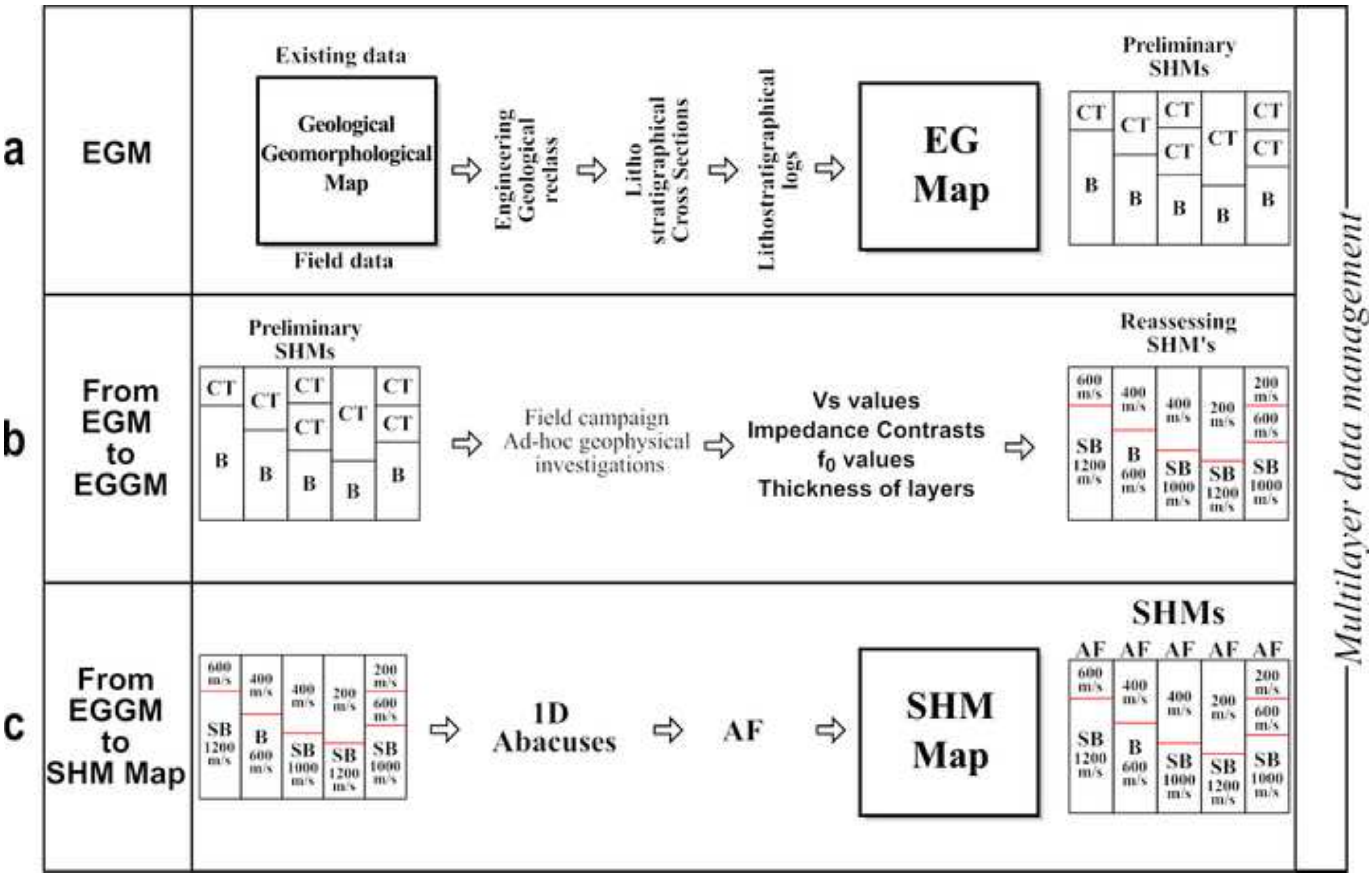

Figure 2

Click here to access/download;Figure;Fig_2.jpg

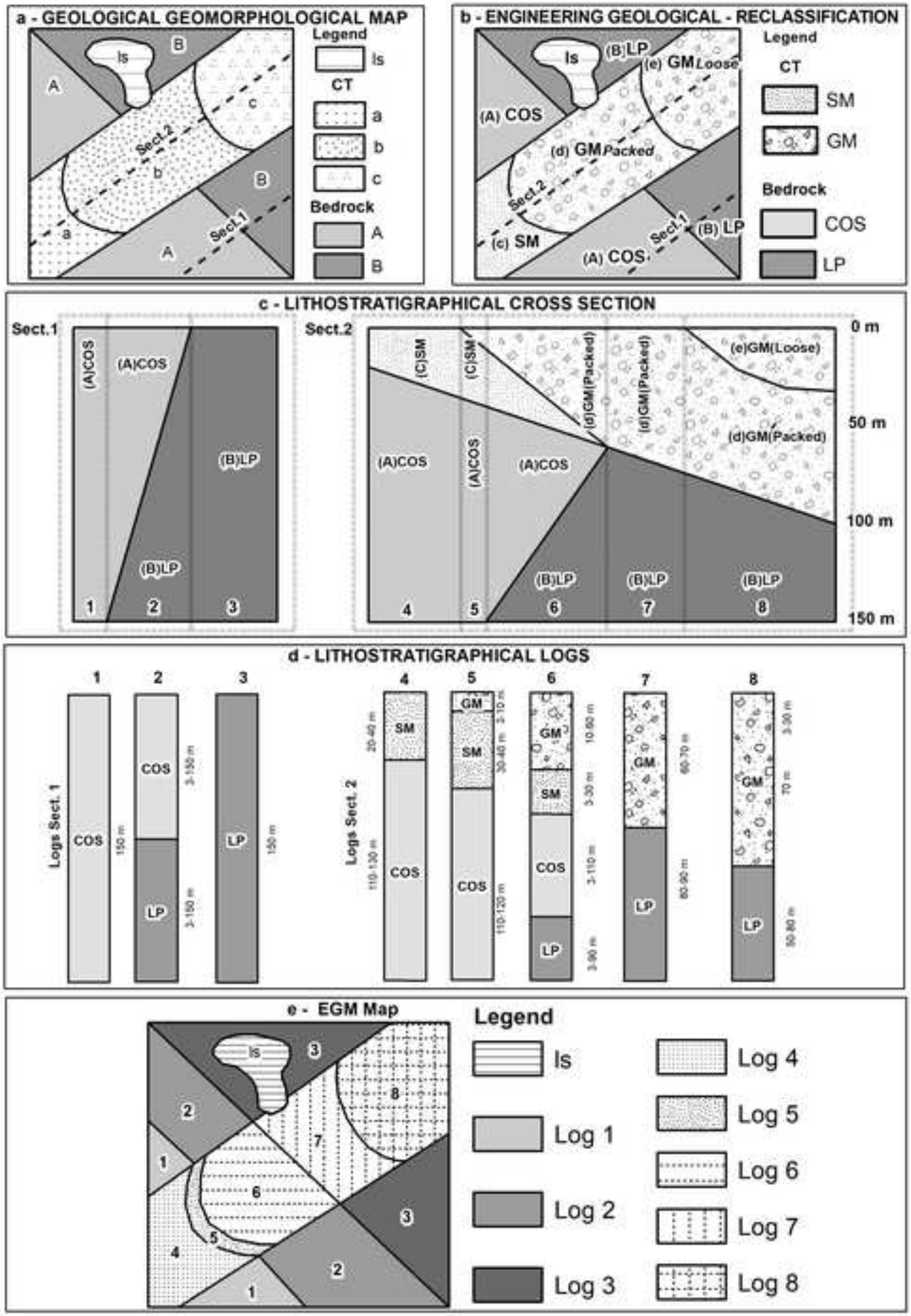

Figure 3

Click here to access/download;Figure;FIG_3.jpg

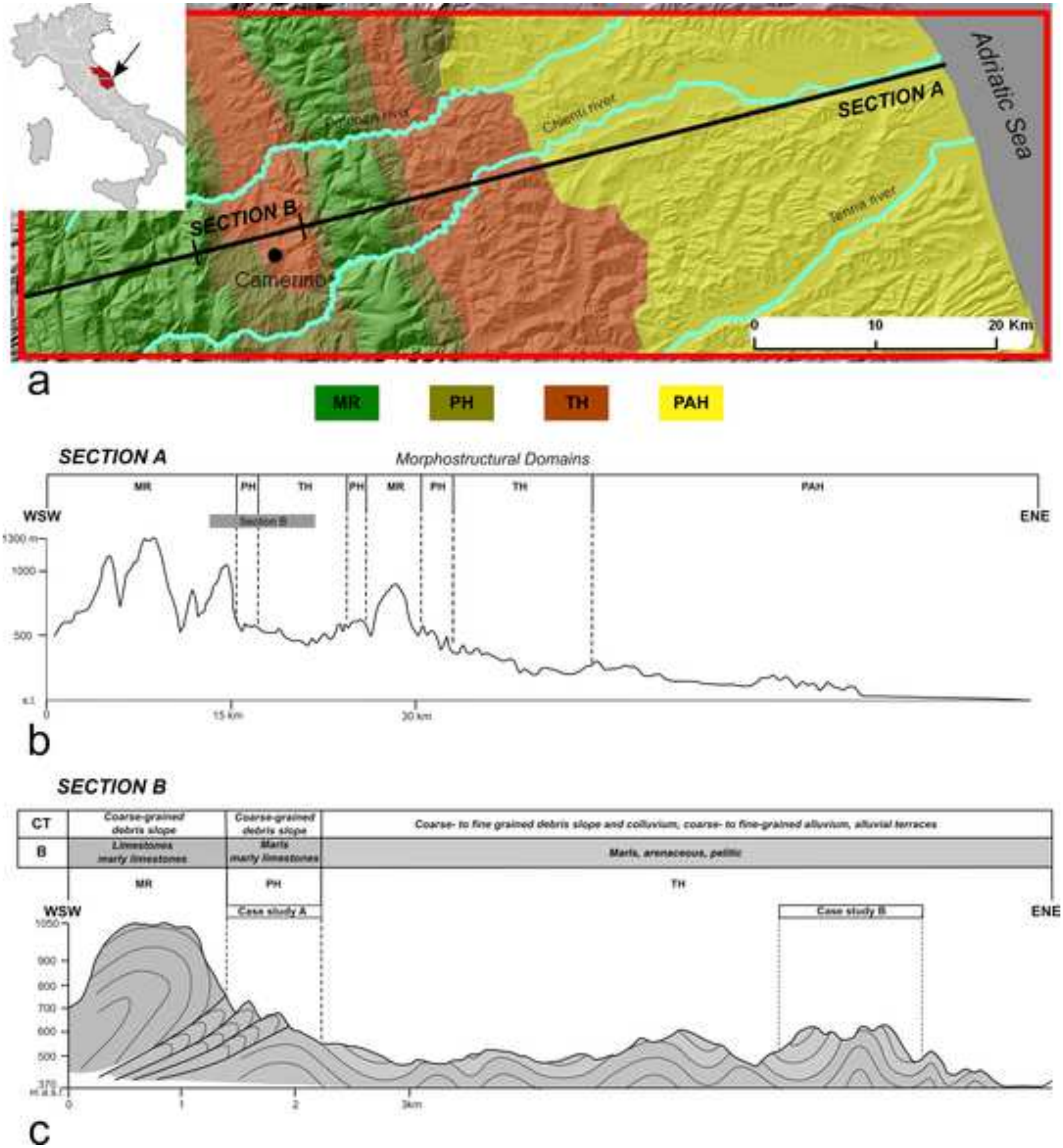

Figure 5

Click here to access/download;Figure;FIG_5.jpg

SE - S.ERASMO

log id	Min (m)	Max (m)	B/CT	gt code	Description
1	2	5	CT	ML	Unsorted low plasticity silts, clays and sands
1	30	140	B	COS	Marls and clays (SCH Fm)
1	10	70	B	ALS	Marly limestones (BIS Fm)
2	5	25	CT	GP	Angular to subangular unsorted calcareous debris-slope, weakly to strongly cemented
2			B	COS	Marls and clays (SCH Fm)

AR - ARNANO

log id	Min (m)	Max (m)	B/CT	gt code	Description
1	5	20	CT	GP	Angular to subangular unsorted calcareous debris-slope, weakly to strongly cemented
1			B	ALS	Limestones and marls (SCC Fm)

CA - CALCINA

log id	Min (m)	Max (m)	B/CT	gt code	Description
1	70	100	B	ALS	Marly limestones (BIS Fm)
1	10	20	B	COS	Marls and clays (SCH Fm)
1	5	30	B	ALS	Marly limestones (BIS Fm)
2	5	25	CT	GP	Angular to subangular unsorted calcareous debris-slope, weakly to strongly cemented
2			B	ALS	Marly limestones (BIS Fm)
3	5	15	CT	GP	Angular to subangular, loose, unsorted calcareous debris
3	5	25	CT	GP	Angular to subangular unsorted calcareous debris-slope, weakly to strongly cemented
3			B	ALS	Marly limestones (BIS Fm)

SM - S.MARCELLO

log id	Min (m)	Max (m)	B/CT	gt code	Description
1	3	10	CT	ML	Holocene fine-grained usnorted eluvial and colluvial deposits
	3	15	CT	GM	Pleistocene alluvial packed unsorted gravels and sands
			B	COS	Marls and clays (SCH Fm)

log id	Min (m)	Max (m)	B/CT	gt code	Description
2			B	COS	Marls and clays (SCH Fm)

log id	Min (m)	Max (m)	B/CT	gt code	Description
3	3	10	CT	ML	Holocene fine-grained usnorted eluvial and colluvial deposits
			B	COS	Marls and clays (SCH Fm)

SN - SENTINO

log id	Min (m)	Max (m)	B/CT	gt code	Description
1	3	50	B	GRS	Arenaceous lithofacies (FCld Fm)
	15	15	B	COS	Pelitic-arenaceous lithofacies (FCk Fm)
	3	30	B	GRS	Arenaceous lithofacies (FCld Fm)
			B	COS	Marls and clays (SCH Fm)

SS - S.SILVESTRO

log id	Min (m)	Max (m)	B/CT	gt code	Description
1			B	COS	Marls and clays (SCH Fm)

log id	Min (m)	Max (m)	B/CT	gt code	Description
2	3	100	B	GRS	Arenaceous lithofacies (FCld Fm)
			B	COS	Marls and clays (SCH Fm)

Figure 8

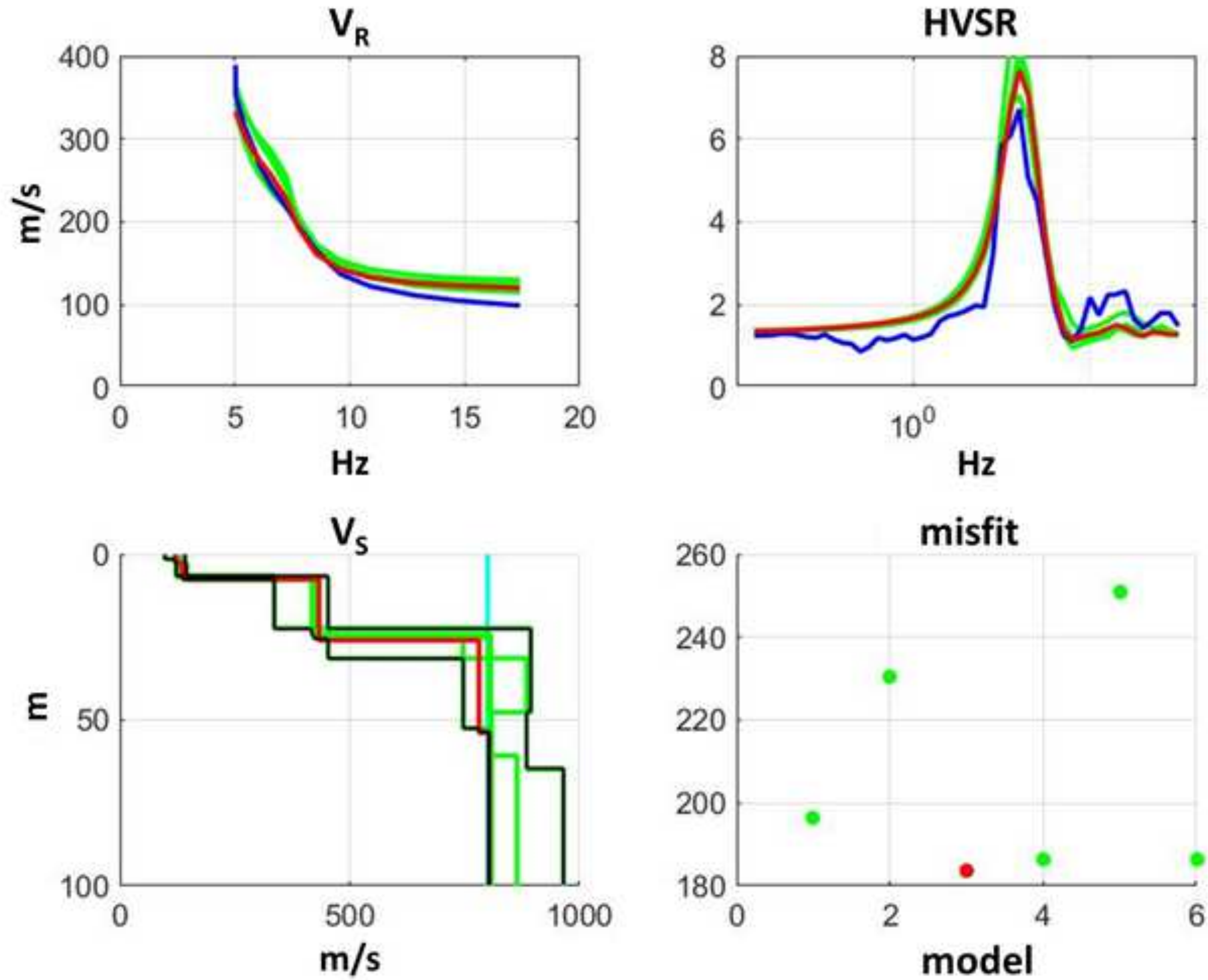

V_R
m/s
400
300
200
100
0
0
5
10
15
20
Hz
HVSR
8
6
4
2
0
10^0
Hz
V_S
0
50
100
m
0
500
1000
m/s
misfit
260
240
220
200
180
0
2
4
6
model

SE - S.Erasmo

log id	EGM Min (m)	EGM Max (m)	EGM B/CT	EGM gt code	EGGM Min (m)	EGGM Max(m)	Vs min (m/s)	Vs max (m/s)	B-SB-CT	gt code
1	2	5	CT	ML	3	5	300	300	CT	ML
	30	140	B	COS	4	6	220	290	B	COS
					5	8	210	270	B	
					11	17	300	460	B	
	10	70	B	ALS			730	870	SB	ALS

SE - S.Erasmo

log id	EGM Min (m)	EGM Max (m)	EGM B/CT	EGM gt code	EGGM Min (m)	EGGM Max(m)	Vs min (m/s)	Vs max (m/s)	B-SB-CT	gt code
2	5	25	CT	GP	3	4	110	130	CT	GP
					5	10	260	350		
			B	COS	10	29	460	750	B	
							820	1200	SB	COS

AR - Arnano

log id	EGM Min (m)	EGM Max(m)	EGM B/CT	EGM gt code	EGGM Min (m)	EGGM Max (m)	Vs min (m/s)	Vs max (m/s)	B-SB-CT	gt code
1	5	20	CT	GP	11	13	390	510	CT	GP
			B	ALS	30	36	720	810	B	
							1250	1750	SB	ALS

CA - Calcina

log id	EGM Min (m)	EGM Max(m)	EGM B/CT	EGM gt code	EGGM Min (m)	EGGM Max(m)	Vs min (m/s)	Vs max (m/s)	B-SB-CT	gt code
1	70	100	B	ALS	3	4	400	440	B	ALS
					8	10	600	700		
					13	30	740	880		
					20	48	1010	1300	SB	ALS
	10	20		COS			1150	1830	SB	COS
	5	30		ALS						ALS

CA - Calcina

log id	EGM Min (m)	EGM Max(m)	EGM B/CT	EGM gt code	EGGM Min (m)	EGGM Max(m)	Vs min (m/s)	Vs max (m/s)	B-SB-CT	gt code
2	5	25	CT	GP	2	2	190	200	CT	GP
					7	11	450	530		
					9	18	590	710		
			B	ALS			900	1100	SB	ALS

CA - Calcina

log id	EGM Min (m)	EGM Max(m)	EGM B/CT	EGM gt code	EGGM Min (m)	EGGM Max(m)	Vs min (m/s)	Vs max (m/s)	B-SB-CT	gt code
3	5	15	CT	GP	2	9	150	350	CT	GP
	5	25	CT	GP	5	22	490	600	CT	GP
			B	ALS			790	980	SB	ALS

Figure 10

SM - S. Marcello

log id	EGM Min (m)	EGM Max (m)	EGM B/CT	EGM gt code	EGGM Min (m)	EGGM Max (m)	EGGM Vs min (m/s)	EGGM Vs max (m/s)	EGGM B-SB-CT	EGGM gt code
1	3	10	CT	ML	1	9	120	190	CT	ML
	3	15	CT	GM	4	14	360	470	CT	GM
			B	COS			800	900	SB	COS
2			B	COS			750	900	SB	COS
3	3	10	CT	ML	6	8	100	145	CT	ML
			B	COS	16	18	340	430	B	COS
							750	900	SB	COS

SS - S.Silvestro

log id	EGM Min (m)	EGM Max (m)	EGM B/CT	EGM gt code	EGGM Min (m)	EGGM Max (m)	EGGM Vs min (m/s)	EGGM Vs max (m/s)	EGGM B-SB-CT	EGGM gt code
1			B	COS			>800	>800	SB	COS
2	3	100	B	GRS	11	12	470	490	B	GRS
					19	28	700	890	B	
			B	COS			900	940	SB	GRS COS

SN - Sentino

log id	EGM Min (m)	EGM Max (m)	EGM B/CT	EGM gt code	EGGM Min (m)	EGGM Max (m)	EGGM Vs min (m/s)	EGGM Vs max (m/s)	EGGM B-SB-CT	EGGM gt code
1	3	50	B	GRS	4	5	280	300	B	GRS
	15	15	B	COS	26	30	450	510	B	
	3	30	B	GRS	24	30	790	900	SB	GRS COS
			B	COS			1390	1500	SB	GRS COS

Figure 11 Color

Click here to access/download;Figure;FIG_11_new.jpg

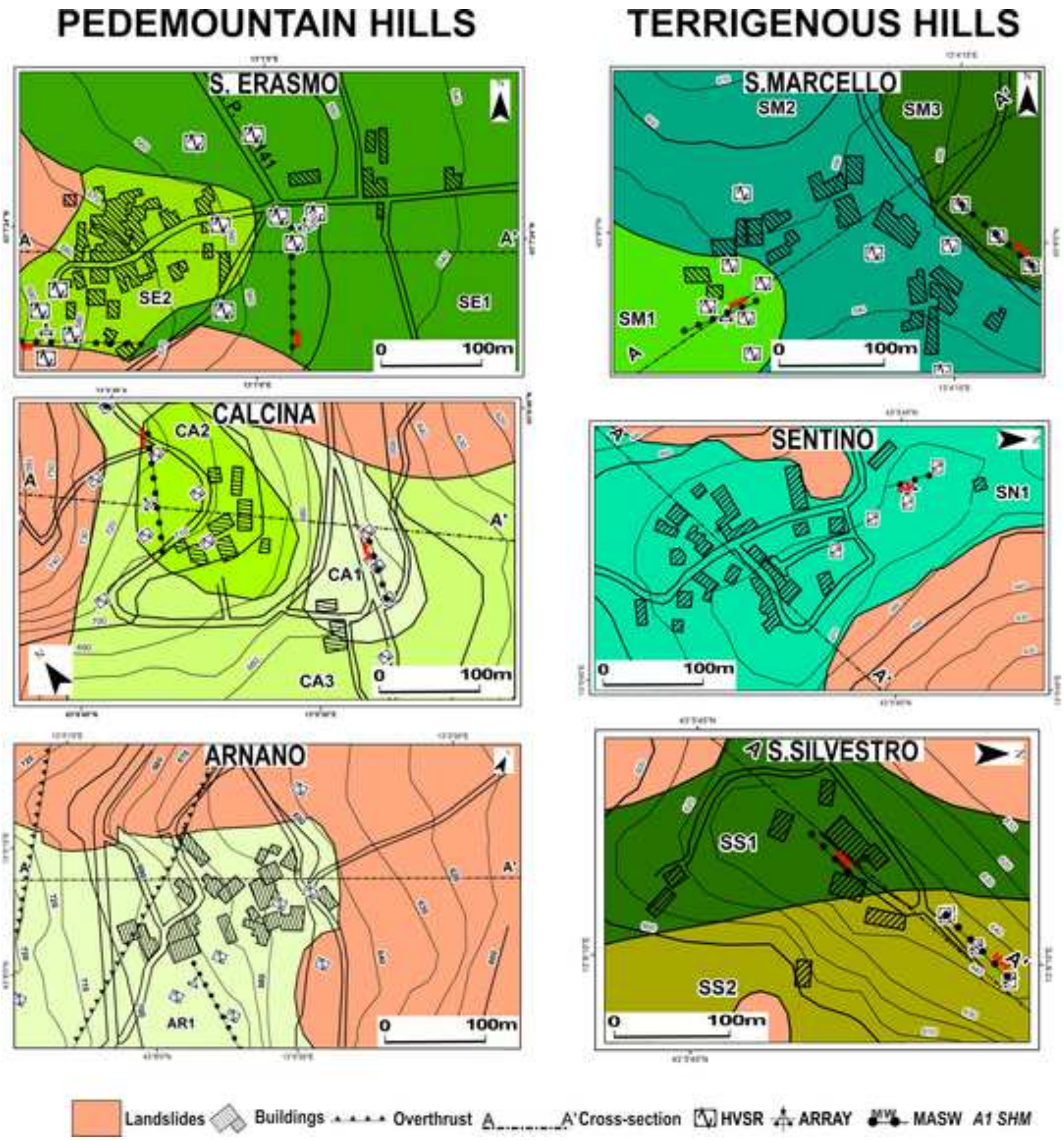

Figure 4 Color

Click here to access/download;Figure;FIG_4_new.jpg

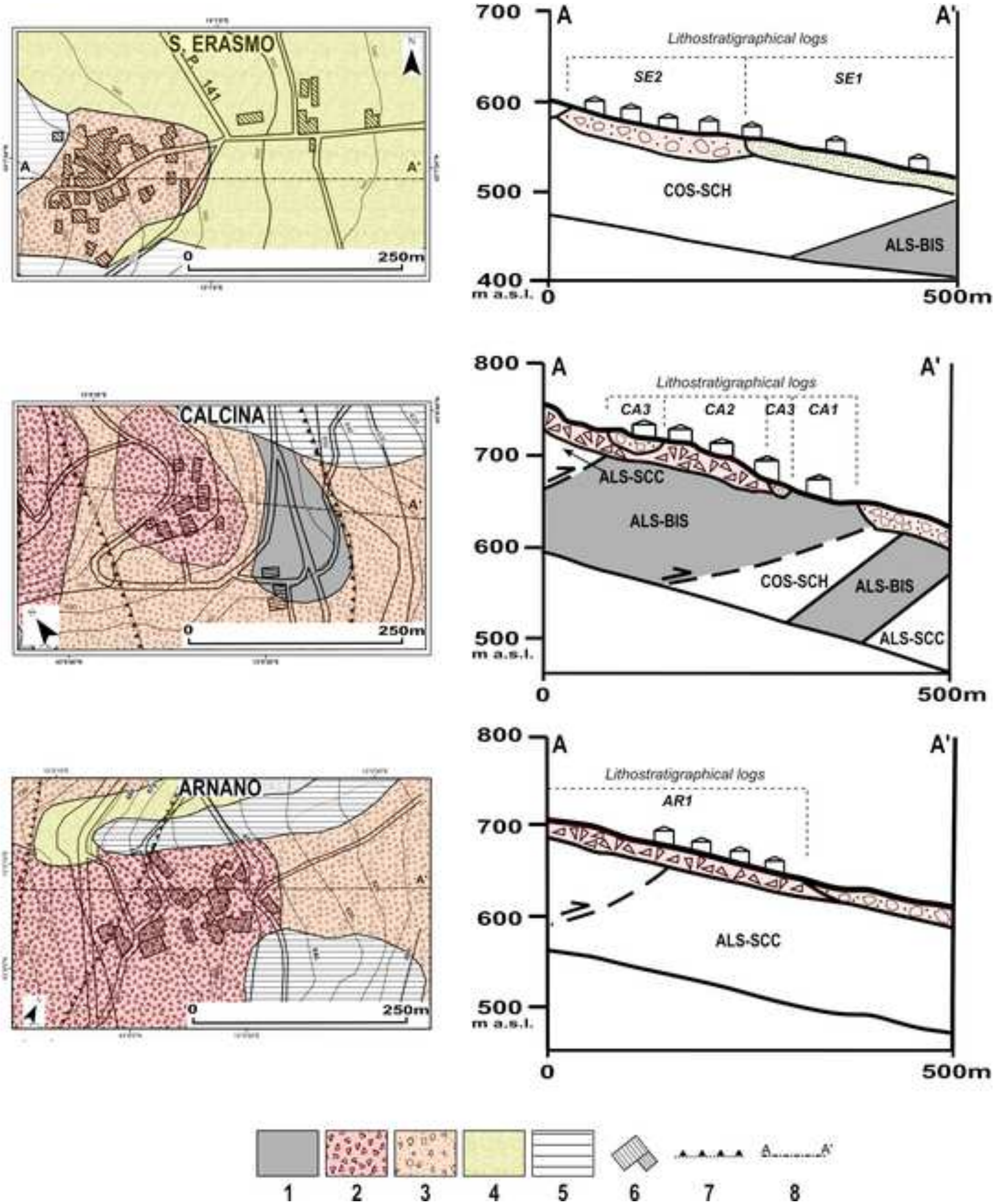

Figure 6 Color

Click here to access/download;Figure;FIG_6_new.jpg